

Near-Infrared Light Brightens Bacterial Disinfection: Recent Progress and Perspectives

Qinyu Han, Jun Wei Lau, Thang Cong Do, Zhijun Zhang,* and Bengang Xing*

Cite This: <https://dx.doi.org/10.1021/acsabm.0c01341>

Read Online

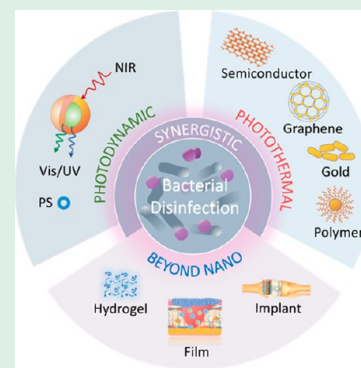
ACCESS |

Metrics & More

Article Recommendations

ABSTRACT: Bacterial infection is a universal threat to public health, which not only causes many serious diseases but also exacerbates the condition of the patients of cancer, pandemic diseases, e.g., COVID-19, and so on. Antibiotic therapy has been used to be an effective way for common bacterial disinfection. However, due to the misuse and abuse of antibiotics, more and more antibiotic-resistant bacteria have emerged as fatal threats to human beings. At present, more than 700,000 patients die every year with bacterial infections because of the lack of effective treatment. It is frustrating that the pace of development of antibiotics lags far behind that of bacterial resistance, with an estimation of 10 million deaths per year from bacterial infections after 2050. Facing such a rigorous challenge, approaches for bacterial disinfection are urgently demanded. The recently developed near-infrared (NIR) light-irradiation-based bacterial disinfection is highly promising to shatter bacterial resistance by employing NIR light-responsive materials as mediums to generate antibacterial factors such as heat, reactive oxygen species (ROS), and so on. This treatment approach is proved to be a potent candidate to accurately realize spatiotemporal control, while effectively eradicating multidrug-resistant bacteria and inhibiting antibiotic resistance. Herein, we summarize the latest progress of NIR light-based bacterial disinfection. Ultimately, current challenges and perspectives in this field are discussed.

KEYWORDS: NIR light, bacterial infection, antibacterial agent, multidrug-resistant bacteria, theranostic, photothermal therapy, photodynamic therapy, light-responsive material



1. INTRODUCTION

Bacterial infection has been a globally deterring threat to human well-being by inducing many diseases such as pneumonia, meningitis, sepsis, cholera, skin ulcer, and gastric cancer, etc. Besides, bacterial infection is a common complication that happens along with cancer, diabetics, and even an infectious pandemic such as COVID-19. Latest research showed that up to 6.9% COVID-19 patients suffered from bacterial infection, which largely aggravates the illness and escalates the difficulty of treatment.¹ The antibiotic which has been prevalently known for a hundred of years is representing a vital line of defense against bacterial infection. Even so, due to the extensive utility of antibiotics in clinics, communities, and agricultural sectors, diverse antibiotic-resistance bacteria are emerging to cause a detrimental catastrophe, posing a greater threat to the population at large than ever before.² The buildup of the antibiotic resistance diminishes the potency of antibiotics, thereby rendering some of severe clinical infections intractable. According to a report from the UN Ad Hoc Interagency Coordination Group on Antimicrobial Resistance, drug-resistant bacterial infection contributes to 700,000 patients' deaths a year at present and the total number of deaths will elevate to 10 million every year from 2050 if urgent concern is not received.³ Innumerable efforts for discovering novel

antibiotics have been executed, yet our ability to discover new antibiotics and combat the evolution of antibiotic resistance in pathogenic microbes is still limited. Most current antibiotics in use to date have been discovered during the prime time for antibiotics invention during the 1940s to 1960s.⁴ In provision for the slow-going antibiotic development and increasing spread of resistance, an unprecedented non-antibiotic approach is urgently needed to be employed to conquer bacterial infectious diseases.⁵

In recent years, with the development of nanosynthesis technology and the cross-fusion of multiple disciplines, many innovative ideas for the treatment of bacterial infection have been afforded.^{6–8} In particular, functional nanomaterials have been widely applied in antimicrobial research as potential drugs.^{9–11} And many of these materials with special properties were found to have greatly enhanced antibacterial activity under external stimulations.¹² For example, using lights, magnetic

Special Issue: Functional Biomaterials for Infectious Diseases

Received: October 15, 2020

Accepted: November 22, 2020

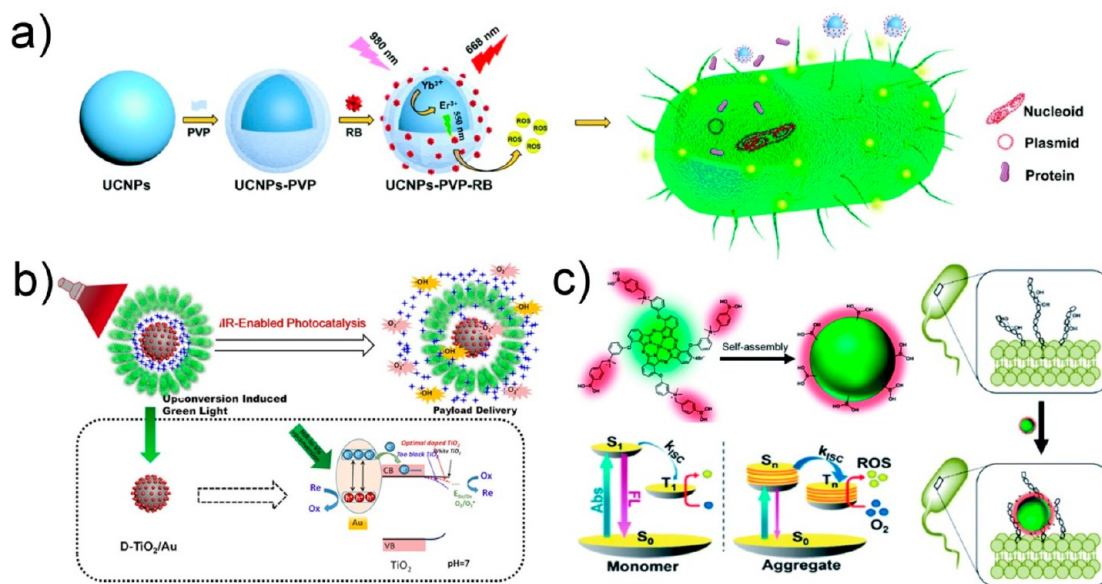


Figure 1. (a) Schematic illustration of the synthesis and antibacterial action of the UCNPs-PVP-RB nanosystem. Reprinted with permission from ref 49. Copyright 2020 Royal Society of Chemistry. (b) NIR light-triggered ROS generation by the D-TiO₂/Au@UCN nanocomposites. Reprinted from ref 52. Copyright 2019 American Chemical Society. (c) Schematic diagram of the self-assembly of PcN4-BA and the antibacterial activity. Reprinted with permission from ref 54. Copyright 2020 Royal Society of Chemistry.

fields, and other physical stimulations, specific materials, such as TiO₂, Fe₃O₄, and graphene, *etc.*, can generate enough heat and free radicals to destroy the structures of bacteria or block the bacterial metabolic pathways to achieve antibacterial effects.^{13,14} Compared to the conventional antibiotic therapy, these physical stimulation based antimicrobial strategies have a broad spectrum of highly effective antibacterial activities against both normal bacteria and multidrug-resistant (MDR) bacteria and an ability to reduce the threat of the burgeoning bacterial drug resistance.^{15–19} Among these physical stimulation strategies, light stimulation, especially near-infrared (NIR) light irradiation, is undoubtedly the best choice in terms of safety, operability, and low cost of apparatus, *etc.*^{20,21} NIR light (700–1300 nm) has the unique advantages of superior tissue depth penetration without resulting apparent photoinduced cytotoxicity, which are conducive to the construction of diverse antibacterial platforms for in-depth treatments.^{22–24} Indeed, strategies, such as photodynamic, photothermal, and synergistic therapeutic modalities that are based on NIR light, have been extensively reported to eliminate bacterial inflammation, thus helping wound healing, promoting tissue regeneration, and so on.^{25–27} These results have unequivocally demonstrated the broad application prospects of NIR-assisted bactericidal strategies and have undoubtedly built up concrete fundamentals in this field. To provide guidance for follow-up research, it is necessary to systematically summarize and review the existing relevant literature. Although many literature reviews have been reported on antimicrobial activities, there has been no systematic review of NIR-assisted antimicrobial strategies.^{28–33} Therefore, in this summary, we will comprehensively review the latest progress regarding NIR-assisted antimicrobial strategies from all aspects of photodynamic, photothermal, synergistic therapies, and the applications of antibacterial medical devices, as well as investigate their prospective developments.

2. PHOTODYNAMIC THERAPY

Photodynamic therapy (PDT) is a propitious alternative to replace traditional antibacterial therapies by offering the advantages of non-invasiveness, low side effects, and target specificity.³⁴ Upon the administration of photosensitizers (PSs), cytotoxic species will be generated under irradiation to rapidly damage the bacterial membrane, oxidize the lipids and the proteins, and finally sterilize the lesion.^{35–37} Generally, under the specific wavelength irradiation, a singlet state electron in a ground state PS (S₀) undergoes an electronic transition to an excited singlet state (S₁). After losing extra energy by vibrational relaxation and internal conversion, the excited electron may undertake an intersystem crossing into a more stable and long-lived excited triplet state (T₁), or lose energy by fluorescence emission (*i.e.*, radiative transition) returning to the ground state. This characteristic property endows most PSs the ability to be used as fluorescence-imaging contrast agents. The PS in the T₁ state may lose the energy by phosphorescence process and undergoes type I reaction in which superoxide anions ([•]O₂[−]) were generated by the electron transfer between T₁ PS and neighboring oxygen to further produce other highly reactive oxygen species (ROS), such as hydroxyl radicals (HO[•]), hydroxide ions (HO[−]), hydrogen peroxides (H₂O₂), singlet oxygen, and peroxyinitrites ([−]OONO), *etc.* Alternatively, the T₁ PS also can undergo type II reaction by transferring energy directly to ground state triplet oxygen (³O₂) to form excited state singlet oxygen (¹O₂) which will induce direct or indirect cytotoxicity to tainted sites, depending on the localization and dose. Notably, the short life and high reactivity of ROS only allow the destruction to surrounding infected tissue within a few nanometers of PS binding sites, resulting in the site specificity of the PDT treatment.³⁸

2.1. Upconversion Nanoparticle. Although possessing robust photodynamic characteristics, common PSs generally require short-wavelength excitation, which significantly restricts their effective medical use in the diagnosis and treatment of superficial bacterial infections due to light spectrum overlap with

optical absorption bands of intrinsic biological tissues. Under such circumstance, NIR irradiation is considered as a promising tool to minimize tissue absorption, scattering, and autofluorescence.^{39,40} In recent research, heartening outcomes have been achieved by utilizing upconversion nanoparticles (UCNPs) as carriers for PSs to convert long-wavelength NIR excitation to short-wavelength visible or UV emission.⁴¹ In UCNP, the long decay time and high probability of sequential excitations of lanthanide caused by the dipole-forbidden nature of the 4f–4f transition will firmly benefit the anti-Stokes emission process (*i.e.*, photon upconversion). Through the multiphoton absorption, emission of light at a shorter wavelength with higher energy than that of excitation light can be attained, allowing the occurrence of the Förster resonance energy transfer (FRET) process to further stimulate the short-wavelength excited PSs for ROS generation.⁴² For instance, the PS curcumin, possessing the singlet oxygen generation ability and inherent antibacterial characteristics, was applied to treat deep joint tissue infection with UCNP as an intermediate carrier. The transition emission of NaYF₄:Yb,Er UCNPs at 450 nm (¹D₂–³F₄) and 475 nm (¹G₄–³H₆) under 980 nm excitation successfully activated curcumin for PDT, thus achieving the eradication of methicillin-resistant *Staphylococcus aureus* (*S. aureus*, MRSA).⁴³

Via matching of the emission spectrum of UCNP and the absorption spectrum of the PS, enhanced tissue penetration of PDT-functional UCNPs was realized by Xu *et al.*, who conjugated the PS Rose Bengal (RB) to the silica (SiO₂) shell of nanoparticles with potent antimicrobial photodynamic effects under 980 nm irradiation.⁴⁴ Likewise, Gruner and co-workers proposed silicon phthalocyanine (SiPc)-loaded silica-coated UCNPs with different surface functionalizations to successfully inactivate bacteria.⁴⁵ Notably, the silica-surface-coating strategy is widely applied to antibacterial nanoagents to enhance their overall liquid dispersibility and biocompatibility.^{46,47} Furthermore, hydrophilic synthetic polymers such as poly(vinylpyrrolidone) (PVP) are also commonly used as coating materials to prevent particle aggregation and to increase the water solubility of nanoparticles.⁴⁸ Liu *et al.* recently introduced a LiYF₄:Yb/Er-based UCNP with RB loading on a PVP coating as a PDT platform, which could accumulate in the periphery of the drug-resistant bacillus *Acinetobacter baumannii* (XDR-AB) in deep tissue (approximately 5 mm) and disrupt the bacterial membrane under 980 nm excitation (Figure 1a).⁴⁹

Compared to homogeneously distributed UCNPs, core–shell UCNPs containing spatially confined dopant ions in the interior markedly enhance the upconversion emission and optical integrity of nanoparticles.⁵⁰ By implementing such an approach, Li and co-workers constructed a cationic antibacterial nanostructure by doping the PS zinc phthalocyanine (ZnPc) into a core–shell upconversion nanoparticle NaYF₄:Yb,Er@NaYF₄ with relatively high upconversion fluorescence efficiency, thus benefiting the efficacy of ROS generation.⁵¹ The multifunctional nanopatform NaYF₄:Yb,Er@NaGdF₄:Nd@SiO₂-RB presented by Xu *et al.* combines PDT, luminescence imaging, and magnetic resonance imaging (MRI) by simply co-doping lanthanide ions Gd³⁺ and Nd³⁺ into the lattice structure of nanoparticles.⁴⁶ In addition to the employment of frequently used PSs, an NIR-photocatalytic antiseptic platform comprising Au/dark-TiO₂ as the core and upconversion nanomaterials as the shell was reported by Xu and co-workers. Under 980 nm excitation, the presented drug-release nanopatform realized PDT antibacterial treatment by inducing high surface plasmon

resonance (SPR) of gold on dark TiO₂ for robust upconversion luminescence (UCL) emission (Figure 1b).⁵²

2.2. Others. As alternatives of UCNP-based platforms converting NIR light to visible light to excite PSs with visible absorbance, materials with one-photon absorption (OPA) or two-photon absorption (TPA) such as NIR-absorbing PSs and NIR-activating quantum dots (QDs) have been developed for in-depth antimicrobial PDT under direct NIR excitation.⁵³ For example, boronic acid-functionalized zinc(II) phthalocyanine (PcN4-BA) for direct NIR-induced bacterial inactivation was introduced by Lee and colleagues, showing significantly augmented ROS generation *via* self-assembly in water with minimal dark toxicity. Interestingly, the boronic acid is commonly applied for the bacterial targeting by covalently binding to diol-containing lipopolysaccharides (LPS) on Gram-negative bacterial surface to form boronic esters (Figure 1c).⁵⁴ Furthermore, NIR-activating graphene quantum dots (GQDs) composed of carbon-based semiconductor nanocrystals with extremely small size (2–10 nm) and good biocompatibility have shown great potential to abolish pathogenic bacteria through ROS generation.⁵⁵ By exploiting NIR-GQD as the NIR-photon PS and the contrast agent coupled with two-photon excitation laser microscopy, Kuo *et al.* reported the complete elimination of MDR strains of pathogens by PDT, and distinct two-photon luminescence (TPL) imaging under 800 nm irradiation with high spatial resolution.⁵⁶ Recently, a heavy-metal-free indium phosphide (InP) QD with narrow band gap, increasing the photoefficacy to kill MDR pathogens, was presented by Levy and his group. The proposed therapeutic QD nanoparticles which could generate superoxide radicals intracellularly were proven to be suitable for NIR-mediated treatment with superb diffusion in microbes and excellent biological compatibility through renal clearance.⁵⁷

3. PHOTOTHERMAL THERAPY

Owning the benefits of PDT, photothermal therapy (PTT) provides specific and non-invasive laser-induced thermotherapy to eradicate the bacteria. The photosensitive agent is able to introduce a thermal ablation to lesion-containing *loci* by photoinduced hyperthermia.²⁵ With photon energy absorption, the electronic transition happens from S₀ to S₁, originating the nonradiative relaxation of instable excited electron to release the kinetic energy as heat, which subsequently denatures the bacterial proteins and causes bacterial death.^{58–60} To be considered as an efficient PTT nanomaterial, the properties of large NIR absorbance, high photothermal conversion efficiency, decent photostability, suitable size, and good biocompatibility should be possessed.⁶¹ Up to now, many valid PTT coupling agents have been discovered, including gold-, carbon-, semiconductor-, polymer- and hybrid-based materials.⁶² Their intrinsic characteristics, recent advancements, and potential defects will be discussed in this section.

3.1. Gold-Based Materials. The noble element gold (Au), at the primordial discovery stage, was renowned for its extreme chemical inertness, as well as possessing superb resistance to oxidation and degeneration.⁶³ In the gradual progress to date, colloidal Au nanoparticles have been widely adopted for their ease of surface fabrication in varied strategies for specifically regulated and targeted therapy. A classical optical phenomenon known as localized surface plasmon resonance (LSPR) is manifested by colloidal Au nanoparticles, in which light of a specific wavelength initiates coherent oscillation of the surface electrons in the conduction band of the Au nanoparticles,

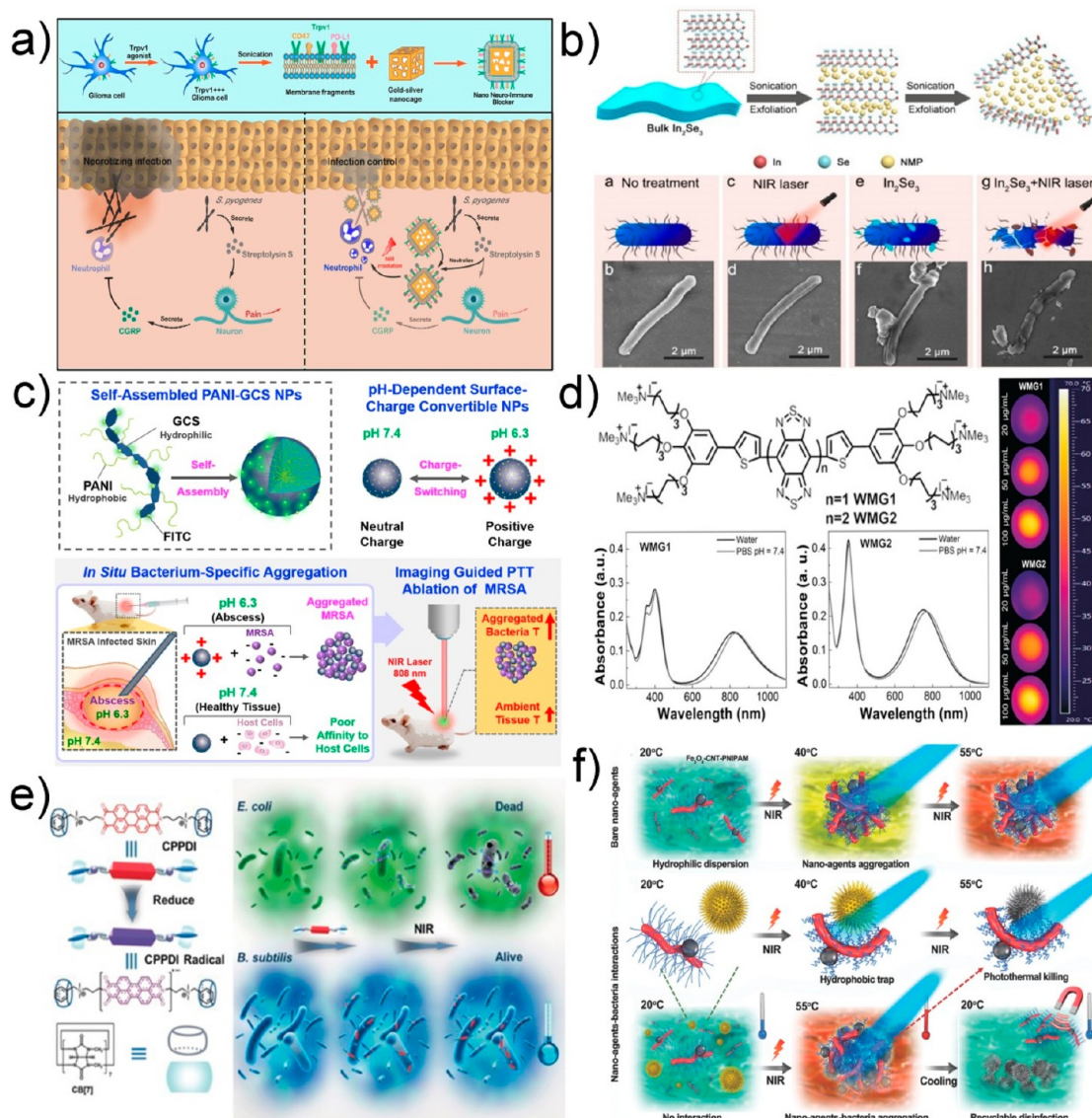


Figure 2. (a) Fabrication and work principle of nano neuro-immune blockers (NNIBs). Reprinted from ref 82. Copyright 2019 American Chemical Society. (b) Schematic illustration of the synthesis of In_2Se_3 nanosheets and the states of *Escherichia coli* (*E. coli*) cells under different conditions. Reprinted with permission from ref 91. Copyright 2018 Wiley-VCH Verlag GmbH & Co. KGaA, Weinheim. (c) Photothermal ablation of focal infections with PANI-GCS NPs self-assembly. Reprinted with permission from ref 102. Copyright 2016 Elsevier Ltd. (d) Structure and photothermal effects of WMG₁ and WMG₂. Reprinted with permission from ref 105. Copyright 2017 Wiley-VCH Verlag GmbH & Co. KGaA, Weinheim. (e) CPPDI showing much higher photothermal disinfection activity toward *E. coli* over *Bacillus subtilis* (*B. subtilis*). Reprinted with permission from ref 107. Copyright 2017 Wiley-VCH Verlag GmbH & Co. KGaA, Weinheim. (f) NIR triggered bacterial disinfection by the Fe_3O_4 -CNT-PNIPAM nanoagents. Reprinted with permission from ref 111. Copyright 2018 Wiley-VCH Verlag GmbH & Co. KGaA, Weinheim.

thereby altering the peak absorption and scattering cross-section, correlated with radiative and nonradiative processes such as absorption, fluorescence, and Raman scattering.^{64,65} To incorporate Au nanoparticles into NIR applications for photothermal therapy and to achieve superior bacteria-targeting potential and biodegradability, the size, shape, and surface modification of the nanoparticles, which are directly related to the LSPR effect, must be significantly optimized to be suitable for adoption in intricate photothermal therapy in the bacterial microenvironment.⁶⁶ In addition, various species of ligands could be used to decorate the surface of Au nanoparticles, vastly augmenting the specificity of treatment without affecting surrounding normal tissues. It has been extensively reported that surface-modified gold nanoparticles have excellent optical absorption efficiency in the NIR optical window with negligible

diminishing effects from the biological medium and tissues, achieving a considerably high ablation effect. Herein, we discuss the diverse materials employed to improve the photothermally induced bacteria killing effect.^{67–72}

Since the presence of various antigens on the surface of bacteria allows the specific formation of antibody–antigen complexes, antibody targeting molecules have been broadly applied to functionalize gold nanoparticles for highly targeted antibacterial responses. Mocan and co-workers biofunctionalized gold nanoparticles with IgG antibodies to achieve selective photoactivated thermal bacterial ablation of MRSA under 808 nm laser power excitation.⁷³ Teng and co-workers effectively treated multidrug-resistant *Pseudomonas aeruginosa* (*P. aeruginosa*) expressing unique secretion protein PcrV by conjugating gold nanocrosses with the primary and secondary antibodies for

protein recognition, followed by the localized photothermal ablation of bacteria under NIR light irradiation.⁷⁴ Adopting the alike strategy, Alhmod and co-workers fabricated gold nanoparticle-decorated porous silicon nanopillars to subsequently conjugate with *S. aureus*-targeting antibody for selective >99% bacterial eradication after 10 min of 808 nm irradiation.⁷⁵ The structural configuration of gold nanoparticles also plays a vital role in photothermal conversion efficiency. As reported by Ocoy and co-workers, gold nanorods excited by 808 nm laser displayed the distinctive hyperthermal bacterial elimination due to the longitudinal SPR band presented in the nanorod shape.⁷⁶ Despite the extensive development of gold nanoparticles, highly sensitive image-guided bacterial ablation is still demanding. Peng *et al.* proposed a poly(ethylene glycol) (PEG)-coated Ag-hybridized Au nanostructure that not only achieved high photothermal conversion efficiency ($\eta = 73\%$) under an 808 nm laser but also enabled sensitive photoacoustic (PA) image-guided bacterial killing *in vivo*.⁷⁷ Du and co-workers developed a FRET-based gelatinase-responsive gold nanostar for NIR fluorescence imaging and localized MRSA photothermal eradication. The nanostar was linked with the NIR fluorescence dye cypate (Cy) by a heptapeptide aptamer linker to form a quenched FRET-based system. Overexpression of gelatinase enzymes in MRSA environment triggers cleavage of the aptamer, thereby releasing the cypate moiety for specific turn-on fluorescence detection and localized photothermal killing.⁸¹ Ma and co-workers replaced commonly used surfactant cetyltrimethylammonium bromide (CTAB) with layered double hydroxides (LDHs) in the synthesis of gold nanorods to increase dispersibility, biocompatibility, and photothermal efficiency. They thus obtained Gold nanorod-LDH-PEG, which is photothermally effective for dual-imaging mode PA- and CT-guided antibacterial and antitumor therapy.⁷⁸ The surfactant CTAB can also be replaced with more biocompatible and less toxic coating agents such as PEG, polyaniline (PANI), and polyethylenimine (PEI) in the synthesis of Au nanoparticles.^{79–81} Furthermore, Au nanoparticles have emerged as a worthy platform to deactivate bacteria by modulating neuroimmune communication. Zhao and co-workers exploited the high expression of transient receptor potential cation channel subfamily V member 1 (TRPV1) and immune escape-related CD47/PD-L1 surface antigens on the glioma cell membrane for the fabrication of gold–silver nanocages. Secreted by *Streptococcus pyogenes* (*St. pyogenes*) bacteria, streptolysin S is responsible for causing pain and releasing sensory neurons to suppress the host immune response, thereby causing necrotizing infection. Since streptolysin S binds well with the TRPV1 ion channel to trigger Ca^{2+} ion influx for neuronal pain conduction, the TRPV1-functionalized Au nanoparticles will specifically target *St. pyogene*, neutralizing streptolysin S to suppress the activation of TRPV1 expressing neurons and thus relieving pain through NIR mediation (Figure 2a).⁸²

3.2. Carbon-Based Materials. Antibacterial nanocarbons, including multiwalled carbon nanotubes (MWCTs), single-walled carbon nanotubes (SWCNTs), and graphene-based nanomaterials (GBNs), have greatly advanced in the past decade for PTT treatment because of their low toxicity, intrinsic thermal conductivity, and high absorption in the NIR region. Notably, despite the advantages possessed by nanocarbons, chemical functionalization is usually required to enhance their colloidal stability and cytocompatibility in physiological environments.⁸³

Graphene derivatives with distinctive two-dimensional sheets have attracted broad research interest, especially as promising candidates for photothermal therapy due to their large surface-to-volume ratio, inexpensive synthesis, and stability characteristics.³⁵ Among them, the graphene oxide (GO) possessing oxygen functional groups (*i.e.*, carboxylic acid, phenol, hydroxyl, and epoxide groups) offers a possibility for stable dispersion formation.⁸⁴ Jia and co-workers used a positively charged chitosan-functionalized magnetic graphene oxide (GO-IO-CS) to inhibit bacterial growth under $2 \text{ W}\cdot\text{cm}^{-2}$ 808 nm irradiation, while introducing a magnetic field efficiently assisting heat localization through controllable bacterial agglomeration and dispersion.⁸⁵ Reduced graphene oxide (rGO) can be obtained by the reaction of reducing agents with GO, decreasing the water stability by eliminating surface oxygen functional groups and increasing the NIR absorbance by restoring π electronic conjugation.⁸⁶ Thanks to its large NIR absorbing cross-section, rGO is successfully used to eradicate the pathogenic bacteria at a laser power density as low as $400 \text{ mW}\cdot\text{cm}^{-2}$.⁸⁷ However, the nanoknife-like feature of GO and rGO may act as a double-edged sword that simultaneously increases antimicrobial efficacy by destroying the bacterial cellular membrane and increases the unexpected normal cell death by piercing the host cell membrane.⁸³ To alleviate these defects, carboxyl graphene (CG) with negligible dark toxicity was designed for improved therapeutic effects *in vivo*. Qian *et al.* presented a pH-responsive glycol chitosan-functionalized carboxyl graphene (GCS-CG) to achieve specific targeting of bacterial infectious lesions in an acidic microenvironment (*i.e.*, pH 6.4), thus realizing precise NIR-based photothermal ablation, which may shed light on the future development of PTT probes for bacterial killing.⁸⁸

3.3. Metal Oxides, Sulfides, Selenides, and Carbides.

Some metal oxides, sulfides, selenides, and carbides, such as Fe_3O_4 , $\text{W}_{18}\text{O}_{49}$, MoS_2 , CuS , In_2Se_3 , Cu_2Se , and Fe_5C_2 , were also found to exhibit great potential in optoelectronics and theranostics due to their large surface area and facile surface modification. In addition, their high photothermal conversion efficiency provided by the large band gap along with broad absorption across the spectrum render them to be reliable candidates for NIR-induced antibacterial treatment.^{89,90} Recently, a liquid exfoliation approach to synthesize 2D $\alpha\text{-In}_2\text{Se}_3$ nanosheets was developed by Zhu and co-workers for large-scale bacteriostatic agent production (Figure 2b).⁹¹ Furthermore, Zhao *et al.* proposed water-dispersible cuprous selenide nanosheets (Cu_2Se NSs) with high photothermal conversion efficiency of up to 61.16% to effectively inhibit the growth of both Gram-negative and Gram-positive bacteria under NIR-II (*i.e.*, 1064 nm) laser irradiation.⁹² Considering their concentration-dependent photothermal conversion capabilities, the antibacterial performance of PTT 2D materials can be further enhanced by fabricating inorganic nanoparticles.⁹³ In addition, magnetic inorganic materials have drawn attention from scientists for use in treating bacterial infections. Both iron oxide nanoparticles and iron carbide nanoparticles possess a paramagnetic nature that enables the fast clearance and recycling of nanocomposites by applying a magnetic field *in vitro* for antibacterial treatments.^{94,95} Moreover, macro-biomolecule-encapsulated inorganic nanoparticles were recently reported to treat pathogenic microbes successfully with great biocompatibility *in vitro*.⁹⁶

3.4. Polymer-Based Materials. Owing to excellent conducting property, photostability, relatively low synthesis expense, and high quantum yield, diverse polymers were

explored in the field of light therapy. Since various supramolecular polymers and polymer-based nanoparticles have been employed for photothermal antibacterial treatment,⁹⁷ this section is presented to introduce the applications of supramolecular polymer structures for bacteria killing upon NIR light activation.

π -conjugated polymer nanoparticles (CPNs) are often considered appealing as they possess enormous π -conjugated backbones and delocalized electronic structure for large extinction coefficients and good light-harvesting activity.⁹⁸ The formation of CPNs often leads to the red shifting for both absorption and emission spectra by high-order aggregation and by energy transfer to the lower-energy emitting sites, thus enabling the NIR application for thorough bacteria eradication. Wang *et al.* adopted a CPN functionalized with positively charged targeting peptide (e.g., Tat peptide) that enabled the formation of CPNs-Tat/bacteria aggregation by interacting with the negatively charged outer membrane of bacteria, achieving a localized heat ablation of bacteria under NIR excitation.⁹⁹ PANI, as a generic conducting polymer used to date, is also commonly employed due to its efficient electronic conductivity, high stability, and high photothermal conversion efficiency when doped under acidic conditions.¹⁰⁰ Abel and his group functionalized PANI with dansyl chloride as the extrinsic fluorophore. The fluorescence detection accompanied by the NIR-induced photothermal treatment ensured a direct and reliable *P. aeruginosa* eradication under 785 nm excitation.¹⁰¹ Similarly, a fluorophore-modified pH-responsive PANI nanoparticle system adopted by Korupalli and co-workers is able to achieve a more localized and enhanced focal photothermal ablation effect. The region of abscesses possessing low pH triggered the chitosan to be positively charged, facilitating a strong electrostatic interaction for *in situ* aggregation with surface-negative bacteria, while the healthy tissue at normal pH was left unaffected. The image-guided PTT with precise abscess treatment ensured the spatial accuracy and targeted heating to the aggregated bacteria upon NIR exposure (Figure 2c).¹⁰² Besides, it was reported that the conjugated polymer with advanced donor–acceptor–donor strategy could attain higher photothermal conversion efficiency due to its lower rate of intersystem crossing, and its high electrostatic potential distributions could afford low-fluorescence radiative transition rate upon interaction with water.^{103,104} Following, Wang and co-workers integrated electron-rich thiophene and electron-poor subunits to give a NIR-shifted charge-transferred conjugated oligoelectrolyte which showed relatively high photothermal conversion efficiency of up to 60%. However, the high heat generation and the toxicity of the conjugated oligoelectrolyte might potentially be setbacks with regard to the nonspecific heat induction and cytotoxicity (Figure 2d).¹⁰⁵ Similarly, Jiao *et al.* discovered a free radical–photothermal correlated strategy to enhance photothermal conversion. As the perylene diimide (PDI) exhibiting a strong π – π interaction which suppresses the supramolecular dimerization and quenches the radical anions, cucurbit[*n*]urils (CB[*n*]) was incorporated to boost the PTT conversion by increasing free radical yield in aqueous solution through sterically hindering the hydrophobic stacking of PDI. The research group found out that the PDI noncovalently attached to the CB[*n*] could achieve improved NIR photothermal conversion efficiency due to the elevation of supramolecular free radicals upon addition of sodium dithionite reducing agent.¹⁰⁶ Following which, this research group exploited this approach to realize the bacteria-responsive photothermal therapy. It is expected that the bacteria

with greater reducing ability could selectively induce more supramolecular free radicals, initiating higher heat generation to be thermally ablated. Comparison was made among *Enterococcus faecalis* (*E. faecalis*), *E. coli*, *S. aureus*, *Bacillus subtilis* (*B. subtilis*), and *P. aeruginosa*, and they reported that facultative anaerobes such as *E. faecalis* and *E. coli* possess more hydrogenases on the membrane, thereby prompting higher reduction rate for free radical formation and NIR photothermal-induced bactericidal effect (Figure 2e).¹⁰⁷

3.5. Hybrid Materials. Compared with single nanoparticles, NIR-responsive hybrid nanoparticles constructed by inorganic and organic components have recently witnessed enormous developments due to their tuning characteristics of different functionalities to minimize the drawbacks of each single component and retain the different beneficial features from all of the components.¹⁰⁸ While organic nanoplateforms can be used as highly biocompatible materials with facile chemical modifications for phototherapy, their stability and light energy conversion efficiency normally hinder their applications. In contrast, inorganic nanoparticles with excellent physical strengths and varied light-response mechanisms can provide relatively stable, tunable, and effective photonic bacterial monitoring, but suffer from poor biodegradability. By integrating the two, the hybrid nanosystem can not only exploit individual strengths but also diminish the weaknesses of each component.

Taking advantage of the excellent NIR absorption ability and high photothermal conversion efficiency of pegylated reduced graphene oxide nanoparticles (rGO-PEG) and gold nanorods (Au NRs), nanohybrid rGO-PEG-Au NRs were developed to effectively irradiate Gram-negative pathogens.¹⁰⁹ As a highly efficient NIR light absorber, polydopamine (PDA) has also been applied as a photothermal agent for the ablation of bacteria. In a recent study reported by Liu *et al.*, the polymer was coated on the surface of the magnetic core Fe₃O₄ to generate a hybrid nanoplateform for the reduction and removal of bacteria. Notably, the loaded HSP70 inhibitor (PES) greatly enhanced the treatment efficacy by breaking the protective function of HSP70 in bacteria.¹¹⁰ Yang *et al.* reported a dual-responsive nanosystem capable of trapping, ablating, and releasing pathogenic bacteria under NIR light monitoring. In this system, temperature-sensitive poly(*N*-isopropylacrylamide) (PNIPAM) was conjugated on the hybrid carbon nanotube (CNT)-Fe₃O₄ surface. Upon NIR light irradiation, the heat generated from the nanohybrid changed the polymer to a hydrophobic form, which therefore promoted the adhesion to the bacterial surface to generate an enhanced photothermal bacteria ablation. Moreover, the result from *in vivo* experiments showed nearly 100% sterilization of the nanoagent-treated mouse wound after PTT with no scabbing from skin inflammation (Figure 2f).¹¹¹

3.6. UCNP-Based Materials. To attain bifunctional modalities for bioimaging and antibacterial photothermal effect, UCNP is being utilized as a potential platform to achieve a precisely monitored bacterial ablation. The trivalent lanthanide ions enclosed in a selected inorganic host lattice enable the sequential absorption of multiple long-lifetime photons on ladder-like energy levels to generate high anti-Stokes luminescence. As mentioned previously, the primary forbidden nature of 4f–4f transition offers a very long lifetime for the excited ion to experience sequential excitations and disparate pathways for ion–ion interactions and energy transfer (*i.e.*, excited state absorption, energy transfer upconversion, cooperative sensitization upconversion, cross-relaxation, and photon avalanche).¹¹²

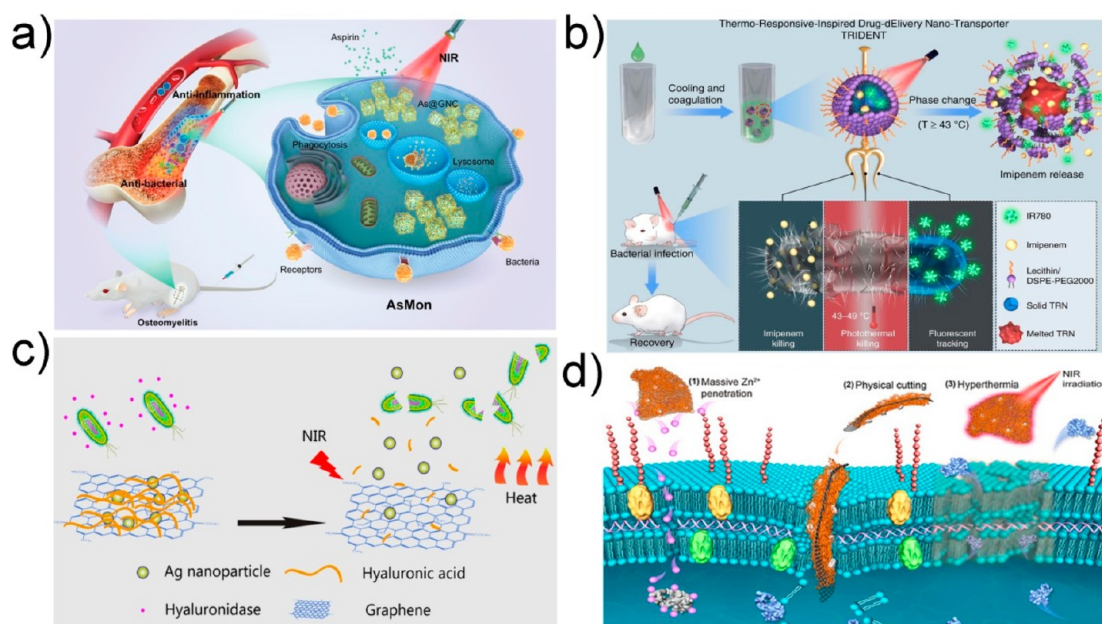


Figure 3. (a) Schematic diagram of the *in vivo* therapeutic effect of aspirin-laden monocytes on osteomyelitis. Reprinted with permission from ref 142. Copyright 2020 Wiley-VCH Verlag GmbH & Co. KGaA, Weinheim. (b) NIR light-activated TRIDENT for antibiotic-resistant bacteria treatment. Reprinted with permission from ref 139. Copyright 2019 The Author(s) under Creative Commons Attribution 4.0 International License (<https://creativecommons.org/licenses/by/4.0/>). (c) Synergistic therapy of bacterial infection by Ag nanoparticles/graphene oxide nanocomposites. Reprinted with permission from ref 153. Copyright 2017 American Chemical Society. (d) NIR-induced 2D-CNs-bacteria aggregation for localized triple bacterial eradication. Reprinted with permission from ref 160. Copyright 2019 American Chemical Society.

These concomitant wave functions of $4f-4f$ transition within a single lanthanide ion thus allow the upconversion photoluminescence to occur with high resistance toward photobleaching and photochemical degradation.^{113,114} In order to advance a UCNP with improved upconversion luminescence, proper surface passivation could be applied to provide an optimal space for energy migration without reaching the outer layer of UCNP and generating surface-related quenching effect.^{115–117} Due to their enhanced photostability, flexible tunability, and low autofluorescence, as well as easy surface functionalization for different therapeutical strategies, UCNPs have often been applied in bioimaging-assisted photothermal therapy. This section reviews the usage of UCNPs for their intrinsic imaging properties and potential heat released abilities to accomplish dual-modal detection and photothermic bacteria ablation.

Suo *et al.* developed thermal sensing and optical heating bifunctional yolk–shell GdOF:Nd³⁺/Yb³⁺/Er³⁺@SiO₂ UCNP-based microcapsules *via* yolk–shell configuration and Nd³⁺, both contributing to a certain extent to the heating property. Internal space between the core and shell due to the yolk–shell shape allows the enhanced energy absorption as well as multiple reflections of NIR light within the cavity, thus enabling an augmented rate of the nonradiative process to generate heat. Excitation of Nd³⁺ ions with 808 nm could enable the photon absorption to be converted to heat due to their metastable multi-intermediate levels with relatively small energy gaps. Most importantly, the subcutaneous temperature increase could be real-time-monitored through the fluorescence intensity ratio (FIR) technique for precise bacterial photothermal ablation.¹¹⁸ Similarly, the same group synthesized a 808 nm light-driven dual-functional olive-like nanoplatfrom LuVO₄:Nd³⁺/Yb³⁺/Er³⁺@SiO₂@Cu₂S with LuVO₄-tridoped nanoparticles as the thermal-sensing core and ultrasamll Cu₂S nanoparticles as the

photothermal agent. Upon 808 nm laser excitation, two disparate green emissions and NIR emission were observed. Thermal-sensing behaviors of samples ($S_a \sim 0.0122 \text{ K}^{-1}$, $S_r \sim 1.4\% \text{ K}^{-1}$) were evaluated on the basis of the high-purity Er³⁺ green emissions, whereas the laser induction at 808 nm intensified with the generated NIR emission that invoked an augmented photothermal ablation efficiency of samples against bacteria *E. coli* and *S. aureus* ($\sim 95\%$).¹¹⁹ Furthermore, Zhang and co-workers developed a nano-photothermal platform with NIR excitation to NIR emission with the design of Y₂O₃:Nd³⁺/Yb³⁺@SiO₂@Cu₂S. This platform encompasses a similar imaging-assisted photothermal induction strategy by adopting the use of Cu₂S as photothermal agent and Nd³⁺ for its heat conversion by nonradiative process for NIR-induced photothermal bacterial ablation.¹²⁰

4. SYNERGISTIC THERAPY

There has been a proceeding effort on alleviating the severity of drug-resistant bacteria by monotherapies such as PTT, PDT, chemotherapy, and others. Nonetheless, the application of monotherapies for bacteria ablation often necessitate the vigorous therapy condition, causing the unavoidable issues such as overheating that are a potential detriment to the surrounding healthy tissues. Optimally, the most facile and safe approach is to integrate a non-invasive, spatiotemporally controlled therapy to leave the healthy cells unscathed. Hence, to effectuate the aforementioned criteria, this review section refers to the achievements of synergistic therapy combined with the merits of various single therapies.^{121–131}

4.1. PTT-Prodrugs. The modest amount of NIR-induced photothermal effect could substantially demolish the bacterial cell membrane and subject it to higher susceptibility, which create an available space for chemodrug-PTT synergistic treatment and lead to greater antimicrobial efficiency.¹³²

Recently, Zhang *et al.* reported a transition metal dichalcogenide (TMD) nanosheet loaded with penicillin for photothermal release of penicillin.¹³³ Zhao and co-workers prepared a NIR-activated thermosensitive phospholipid, distearylphosphatidylcholine (DSPC), and a quaternized cholesterol for bacterial membrane surface targeting to form liposomes, which are then encapsulated with tobramycin and cypate (NIR-sensitive photothermal agent). Positively charged liposome targeted the biofilm and infiltrated the 200 μm wide biofilm microchannel, realizing the antibiotic release upon NIR light treatment to eliminate the biofilm.¹³⁴ Likewise, Zhang *et al.* introduced a thermally sensitive liposome compacted with black phosphorus quantum dots and vancomycin antibiotic, in order to achieve a photothermal/pharmacosynergistic therapy against methicillin-resistant *S. aureus*.¹³⁵ Intriguingly, the same group incorporated an improved photoresponsive antibiotic-releasing strategy through dual thermosensitive gatekeepers, phase-change material (PCM) and poly(*N*-isopropylacrylamide-co-diethylaminoethyl methacrylate) (PND). Upon 808 nm NIR light activation, PCM and PND were provoked by external stimuli PTT to cause the phase transition from solid to liquid and the shrinking conformation for on-demand drug release, respectively. The undesirable drug leakage can be collectively prevented by solid PCM and PND with expanding coil conformation without NIR irradiation.¹³⁶ Besides, Wang and co-workers loaded the thermosensitive 1-tetradecanol (TD) into the hollow interior of the sea urchin-like Bi_2S_3 nanostructures to construct TD/Linalool@ Bi_2S_3 composites for the photothermal controlled release of antibacterial agent.¹³⁷ Compellingly, Wang *et al.* demonstrated a new targeting delivery nanoplatfrom by utilizing a macrophage membrane coated gold–silver nanocage for selective bacteria targeting. Upon pretreatment of macrophage with bacteria, the upregulation of pathogen-related receptors was observed and the macrophages with the excess expression of receptors on cell membranes were used for coating of the gold–silver nanocage. By applying such an approach, the nanoplatfrom could easily recognize and adhere to bacteria with a specific recognition site, consecutively activated by NIR light for drug delivery and photothermal response.¹³⁸ To further achieve precise bacterial ablation, Qing *et al.* introduced a thermoresponsive drug delivery and photothermal ablation strategy for microbial annihilation, accompanied by fluorescent tracking. This functionalized system contains imipenem drug, which releases, upon heat-induced phase-change response, thermoresponsive nanostructure as a phase-change material and IR780 as a NIR light–heat converter as well as a fluorescent tracker. Upon heat induction above 43 $^\circ\text{C}$, phase change occurred to release imipenem, which in turn assisted in the photothermal bacteria treatment through the photothermal–chemosynergistic therapy (Figure 3b).¹³⁹

On an innovative drug-releasing approach, Liu *et al.* presented an enzyme-responsive drug delivery strategy to ablate bacteria biofilm with the aid of photothermal synergism. The ascorbic acid prodrug, which was capped with hyaluronic acid (HA) and ciproflaxin-modified molybdenum sulfide, was adapted to a ruthenium core. Upon specific bacterial targeting, the excess expression of the Hyal enzyme at the biofilm site could potentially degrade the hyaluronic acid capping, thereby releasing the ascorbic acid. The photothermal-responsive MoS_2 consequently catalyzed the ascorbic acid to generate radical hydroxyl species to achieve synergistic biofilm elimination.¹⁴⁰ To elaborate on the dual-stimulus-responsive strategy for drug release, He and co-workers integrated two distinctive

bactericides into one platform, by loading the daptomycin onto gold nanorod preconjugated with pH-responsive glycol chitosan and polydopamine coating. Noteworthy, the acidity-triggered charge reversal would aid in the daptomycin release, while co-stimulating by NIR activation for the augmented release of antibiotic and the enhanced bacteria adherence.¹⁴¹ Furthermore, Shi *et al.* exploited monocyte with programmed anti-inflammatory ability and utilized it to realize the programmed bactericidal and the anti-inflammation for osteomyelitis' treatment. In this antibacterial platform, aspirin-laden monocyte (AsMon) was prepared *in situ* spontaneously by directly injecting the aspirin conjugated-gold nanocage into mouse abdominal cavity. Upon contact with the infection site, the monocyte will differentiate into macrophage in response to bacterial attachment. Internalization of bacteria will then occur followed by the clearance of infection through phagocytosis. The aspirin could also be released in control upon NIR-excited PTT response of gold nanocage, which could assist to inhibit inflammation and osteoclastogenesis, improving the rate of bone regeneration after infection (Figure 3a).¹⁴²

4.2. PTT-Metal Ions. Metal ions have been playing pivotal roles in antibacterial activities.^{143–150} The bactericidal mechanism is mainly relying on the interaction between the ions and the thiol groups or other amino acid moieties in bacteria to modify the normal functions of the bacterial metabolism process.¹⁵¹ For instance, previous studies verified that silver ion could facilitate the bacterial potassium ion (K^+) release, thus dysregulating whole cellular activities.¹⁵² Metal elements are not only beneficial for the antimicrobial activity by physically or metabolically dysfunctioning the bacterial physiological processes but also suitable to be employed as stable backbones for the fabrication of stable nanostructures. In particular, metal-element-doped nanostructures could generate significant non-radiative energy as previously mentioned, providing a possibility for dual-functional combined treatments.

Employment of silver ions (Ag^+) is one of the most popular approaches for antibacterial therapies. To fully exploit the synergistic effects from the photothermal material, many silver-based nanomaterials have been fabricated with a significant therapeutics outcome. For example, Ran *et al.* introduced a nanosystem in which the silver nanoparticles (AgNPs) and GO cooperated in the hyaluronidase (HAase)-coated nanomaterial to generate excellent bactericidal effects under NIR light stimulation (Figure 3c).¹⁵³ Continuing with the promising effects of the synergistic strategy, different Ag materials have been successfully collaborated with other 2D platforms to display the broad sterilizing effects from Gram-negative to Gram-positive bacterial infection models.^{154–156} In another example, silica-coated gold–silver nanocages (Au-Ag@SiO_2 NCs) were presented as an encouraging bactericidal candidate.¹⁵⁷ Similarly, Mei and co-workers developed the miniature Au/Ag core–shell nanorods (NRs) for NIR-II-activatable PTT and PA imaging of MRSA infection. Utilizing the NIR-II phototheranostic approach, Au/Ag NRs were efficiently activated by ferricyanide solution and were allowed to continuously release free Ag^+ to eliminate microbes as well as to promote wound healing.¹⁴⁷ In addition, dual release of Ag^+ and Cu^{2+} under the photothermal treatment introduced from AuAgCu_2O nanogel could further effectively damage exposed bacteria, assisting cutaneous chronic wound healing and keratitis treatment.¹⁵⁸

Likewise, PTT bacterial eradication by CuS nanodots was accelerated by combining with Cu^{2+} release. The robust

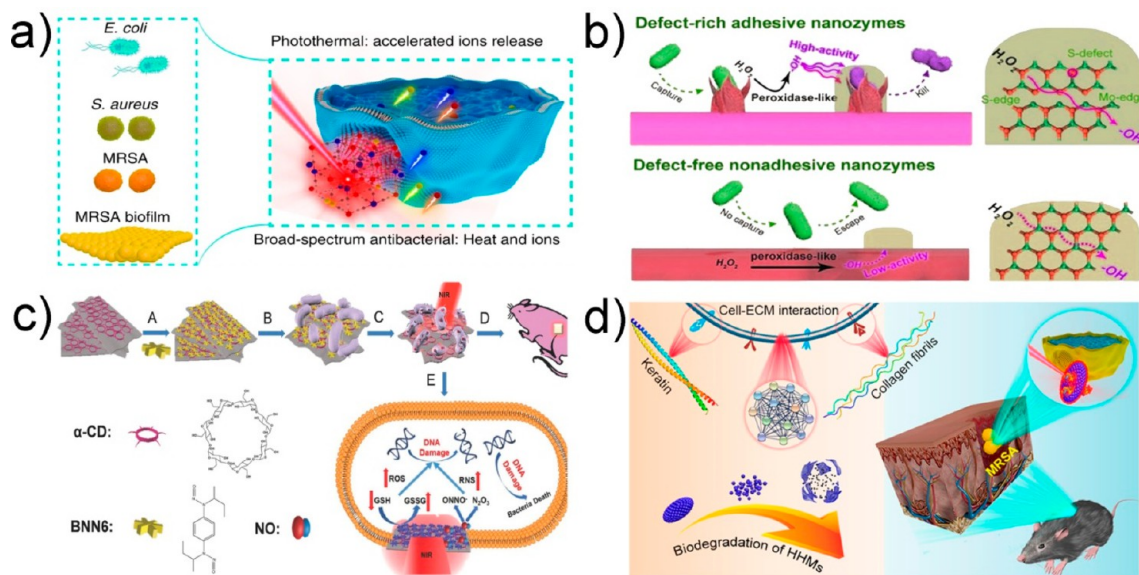


Figure 4. (a) NIR-activated bacterial disinfection by the synergistic effect of heat and ions. Reprinted with permission from ref 162. Copyright 2019 The Author(s) under Creative Commons Attribution 4.0 International License (<https://creativecommons.org/licenses/by/4.0/>). (b) Defect-rich and adhesive nanozymes for enhanced bacterial capture and elimination. Reprinted with permission from ref 168. Copyright 2019 Wiley-VCH Verlag GmbH & Co. KGaA, Weinheim. (c) MoS₂-BNN₆ as NIR laser response NO carrier for synergistic bacteria killing. Reprinted with permission from ref 174. Copyright 2018 Wiley-VCH Verlag GmbH & Co. KGaA, Weinheim. (d) Lysozyme-assisted photothermal eradication of MRSA infection. Reprinted with permission from ref 184. Copyright 2019 American Chemical Society.

induction of the ion in short-period irradiation enhanced the dermal tissue restoration as evaluated in the scratch assay in human foreskin fibroblast cell. Stimulation of the main regulator of oxygen homeostasis, hypoxia-inducible factor (HIF)-1, was observed, and vascular endothelial growth factor (VEGF), a direct neovascularization important factor for wound healing, was also upregulated in the wound area. The results demonstrated by Qiao and co-workers showed the effective therapeutic modality to cure infectious wounds *in vivo* with negligible local or systemic toxicities.¹⁵⁹ Referring to the study by Xu and colleagues, copper-doped calcium silicate bioceramics were introduced to exhibit unique bioactivity based on the release of silicon (Si) ions and Cu ions. The released Cu ions inhibited bacterial growth, while both Si ions and Cu ions can promote angiogenesis and enhance tissue regeneration. Importantly, the alkaline environment created by stimulated the formation of polydopamine which generated the photothermal effect for dual effective antibacterial treatment.¹⁵⁰

Taking advantage of Zn²⁺ ion, the metal–organic framework (MOF) derived from ZnO-doped carbon on graphene (ZnO@G) was fabricated with phase transformable thermally responsive brushes (TRB) by *in situ* polymerization to yield the leveraging 2D structure TRB-ZnO@G with dual-functional antibacterial effects. The NIR light-triggered photothermal effects switched the phase transformation of the polymer and activated the bacterial aggregation process. Meanwhile, the hyperthermia-induced nanostructure enabled Zn²⁺ generation for synergistically enhancing the disruption of bacterial membranes and intracellular substances (Figure 3d).¹⁶⁰ Zeolitic imidazolate framework-8 (ZIF-8) loaded with Zn²⁺ was also utilized as a precursor to obtain bactericidal nanocarbons. Thermosensitive gel layer poly(*N*-isopropylacrylamide) was correspondingly coated on the nanocomplexes to generate localized heat and massive Zn²⁺ for disintegrating bacterial membrane and intracellular proteins.¹⁶¹ Interestingly, doping of zinc ions with variation in levels can tune the space unit of

Prussian Blue (PB) to optimize the bactericidal effect of both PTT and ion release from ZnPB. The mechanism of the enhanced photothermal conversion efficiency of ZnPB is ascribed to the band gap narrowing effect and the red-shifted localized SPR, which move toward lower energies with increasing Zn doping density. Upon NIR light irradiation, the heat generated from the nanosystem disrupted the bacterial membrane and accelerated ion release including Zn²⁺, Fe²⁺, and Fe³⁺ which disturb the metabolic pathways of the bacteria and enhance the bactericidal efficiency. Additionally, the upregulated gene expression (MMP-2, COL-I, and COL-III) and downregulated gene expression (IL-1 β) caused by ZnPB can increase the chemosynthesis of matrix metalloproteinases (MMPs), promote collagen deposition, and inhibit inflammatory factors to favor wound repair (Figure 4a).¹⁶²

4.3. PTT-Nanozymes. Nanozymes, also known as artificially synthetic nanomaterial enzymes, function effectively by imitating the catalytic sites of natural enzymes for diverse catalytic reaction.¹⁶³ Similar to a frequently used natural enzyme peroxidase, the nanomaterial-based peroxidase mimics can catalyze H₂O₂ to generate HO[•], which is an effective antibacterial species. Therefore, nanozymes afford substantial bactericidal ability by catalyzing the H₂O₂ with peroxidase-like activity, bestowing a possible solution to extirpate the bacterial infection combined with photothermal therapy.

To mention a few, Yin *et al.* developed a biomimetic molybdenum disulfide nanoflower functionalized with poly(ethylene glycol) to achieve the catalytic conversion of H₂O₂ to radical hydroxyl species, [•]OH.¹⁶⁴ Huo and co-workers designed a peroxidase-like nanocatalyst that consisted of single iron atoms that were isolated in nitrogen-doped carbon for combating both Gram-negative and Gram-positive bacteria *in vitro*.¹⁶⁵ Besides, Liu *et al.* adopted the nanocatalytic antibacterial therapy and photothermal therapy by implementing hemoglobin-functionalized copper ferrite nanoparticles. The Fenton coupling between the two redox pairs in the nanosystem (Fe²⁺/Fe³⁺

and $\text{Cu}^+/\text{Cu}^{2+}$) can repeatedly catalyze the decomposition of H_2O_2 at a low concentration to generate $\cdot\text{OH}$, which could be further quantified by the oxidation of colorless to chromogenic peroxidase substrate, 3,3',5,5'-tetramethylbenzidine (TMB).¹⁶⁶ Similarly, Li *et al.* introduced a porphyrin-based porous organic polymer ($\text{FePPOP}_{\text{BFPB}}$) which enables the calorimetric detection by TMB and ablation of *S. aureus* by NIR-light-driven photo-Fenton activities.¹⁶⁷ Moreover, Cao *et al.* reported defect-rich adhesive nanozymes by utilizing MoS_2 nanozymes as nanobuilding blocks and copper nanowires as supports. The rough surfaces and defect-rich active edges of nanozymes were designed which not only greatly enhanced the bacterial adhesion but also largely improved the intrinsic peroxidase-like activity *in vitro* and *in vivo* (Figure 4b).¹⁶⁸

4.4. PTT-Gaseous Molecules. Gas therapy has been utilized as an alternative non-invasive treatment for combating bacterial infections lately.^{169,170} Gaseous-signaling molecules (GSMs), including hydrogen (H_2), nitric oxide (NO), sulfur dioxide (SO_2), hydrogen sulfide (H_2S), and carbon monoxide (CO), not only cause negligible side effects to living organisms with high antibacterial capacity but also act as endogenous signal transmitters to induce various biochemical changes in the organism.¹⁷¹

Nitric oxide, as an important molecule involved in the immune responses and wound healing process, has been widely chosen to be cooperative with antibacterial photothermal treatment. The hydrophobic radicals and reactive nitrogen species (RNS) such as nitrogen dioxide (NO_2), dinitrogen trioxide (N_2O_3), and $\cdot\text{OONO}$ generated by NO are responsible for the bacterial DNA deamination and membrane disruption. Yu and co-workers introduced a synergistic strategy by constructing Fe_3O_4 -based magnetic nanoparticles with polydopamine and NO donor *N*-diazoniumdiolate (NONOate). The magnetic characteristic of the presented material successfully assisted the bacterial separation after the NIR light therapy, and the participation of NO endorsed skin regeneration through the increase of myofibroblast and collagen production.¹⁷² Similarly, a versatile magnetic nanoplatform $\text{Fe}_3\text{O}_4@\text{PDA}@\text{Ru-NO}@\text{FA}$ was developed by Liu and his group. The choice of ruthenium nitrosyls as gaseous molecule donor (Ru-NO) endows the platform with low cytotoxicity and appreciable stability for NIR-controllable release in biological tissues.¹⁷³ Qin *et al.* invented a photocontrollable NO-releasing nanovehicle by incorporating 2D TMD photothermal agent MoS_2 and heat-sensitive NO donor *N,N'*-di-*sec*-butyl-*N,N'*-dinitroso-1,4-phenylenediamine (BNN6) to achieve ideal antimicrobial effect. The α -cyclodextrin (α -CD), which consisted of six glucose subunits with hydrophobic cavity and hydrophilic exterior, was modified in the MoS_2 surface, helping the stabilization of the nanosystem. Interestingly, the hyperthermia induced by NIR irradiation to MoS_2 accelerated the process of reduced glutathione (GSH) to oxidized glutathione (GSSG) which further induced the oxidative stress in addition to nitrosative stress, destroying the bacterial structure and cellular function (Figure 4c).¹⁷⁴ In addition, BNN6 could be used to combine with dopamine crafted hydrogel to realize bacteria eradication and wound healing with the minimum leakage of gas.¹⁷⁵

Of late, H_2 gas molecule was recognized as a potential bacteria and biofilm disinfectant by Yu and co-workers. This antioxidant molecule, showing excellent antimicrobial properties by enhancing membrane heat sensitivity, is control-released by palladium nanohydride (PdH) under the 808 nm excitation.¹⁷⁶

4.5. PTT-Cationic Polymers. Photothermal therapy assisted by cationic polymer could greatly enhance the selective targeting toward the negatively charged bacteria surface, which was endowed by teichoic acid and lipopolysaccharide in Gram-positive and Gram-negative bacteria surfaces, respectively. The ease of preparation renders cationic polymer a desirable biomaterial used for surface functionalization, since its properties can be easily modified by various factors including H-bond stabilization, hydrophobic interaction, and polymeric chain flexibility, *etc.*¹⁷⁷ Owing to its beneficial properties, naturally derived or synthetic cationic polymers are prevalently applied in diverse NIR biomaterial applications as we discuss in the section below.

Hu *et al.* presented a pH-responsive Au nanoparticle by conjugating it with two self-assembled monolayers, (10-mercaptodecyl)trimethylammonium bromide ($\text{HS-C}_{10}\text{-N}_4$) and 11-mercaptoundecanoic acid ($\text{HS-C}_{10}\text{-COOH}$). The surface-modified Au nanoparticle exhibited a zwitterionic feature, aggregating with low acidic pH in a bacteria enrichment site while dispersing evenly in normal neutral pH, allowing precise lesion treatment.¹⁷⁸ Feng and co-workers demonstrated an NIR-mediated antimicrobial conjugated polyelectrolyte (CPE) by conjugating with quaternary ammonium (QA). The cationic QA side chain is known to facilitate bacterial recognition and membrane disruption by electrostatic binding. Thus, the synergistic effect of QA and the hyperthermia effect from CPE render the introduced hybrid a potential candidate for photothermal bacterial ablation.¹⁷⁹ Mazrad and co-workers synthesized fluorescent PDA-based carbon nanoparticles passivated with high PEI ratio to acquire a cationic adhesive characteristic to target negatively charged bacterial membranes, providing a decent fluorescence detection by adhesion caused quenching effect and a precise microbial inactivation by photothermolysis.¹⁸⁰ Similarly, by using different surface modifications, Yang *et al.* developed a polypyrrole (PPy)-based photothermal nanomaterial for NIR-II excited bacterial treatment by utilizing the cationic and photothermal properties of PPy.¹⁸¹ Wang *et al.* reported a boronic acid-functionalized graphene-based QA salt to achieve specific bacteria targeting and reduce the damage to the surrounding normal tissues upon sterilization.¹⁸² Attractively, Yang and co-workers conceived a precise luminescent imaging-guided photothermal therapy to improve the spatial accuracy of the bacterial treatment by fabricating PANI and GCS onto the surface of persistent luminescence nanoparticle (PLNP) for selective bacterial binding.¹⁸³ On a disparate bacterial-targeting strategy, Li and co-workers worked on a lysozymes-assisted exogenous killer for NIR-mediated bacterial elimination. Human-hair melanosome derivative (HHM) comprising of melanin as NIR-photothermal-responsive core was grafted with an outer layer of negatively charged keratin, absorbing well with positively charged lysozyme through electrostatic interaction. Notably, this design lies in the biodegradation of HHMs, thereafter undergoing a protein-signaling pathway for the regulation of collagen synthesis to augment tissue repairing wound closure (Figure 4d).¹⁸⁴

4.6. PDT-CHEMO. ROS activities and functions are not limited to causing DNA damage or membrane structure perturbation only; they can also promote the immune responses which are attributable to the wound healing for post-treatment. At the same time, ROS generation from PDT agents is able to stimulate intracellular drug delivery and accelerate drug release in the nanocomplexes.¹⁸⁵ As O_2 is consumed by PDT in the

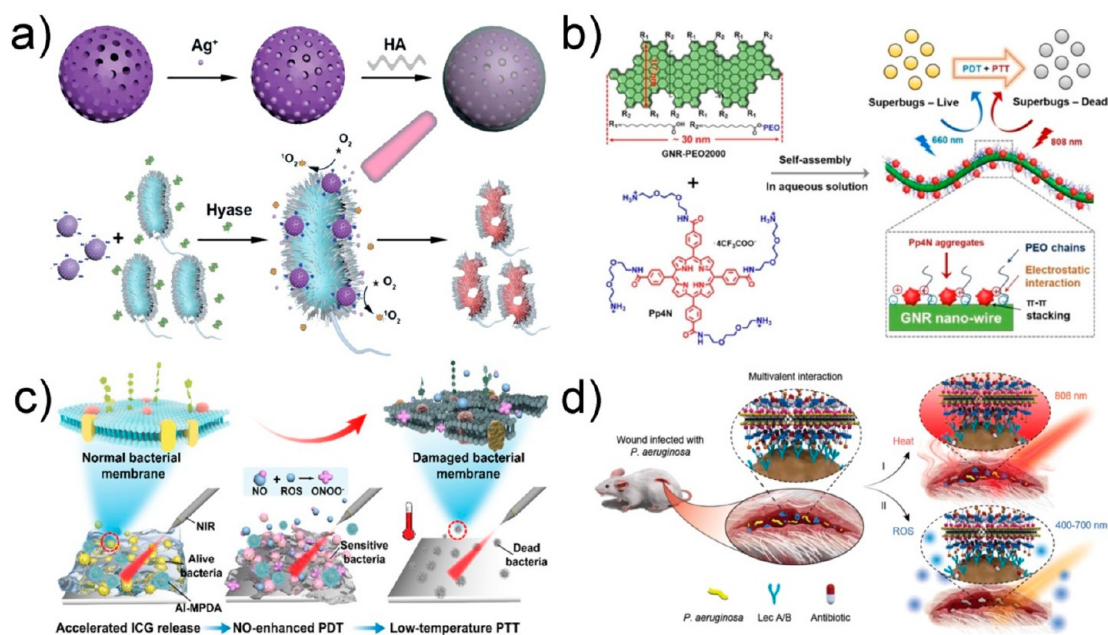


Figure 5. (a) Schematic illustration of the synergistic bacterial disinfection by PCN-224-Ag-HA nanoagents. Reprinted from ref 192. Copyright 2019 Wiley-VCH Verlag GmbH & Co. KGaA, Weinheim. (b) Pp4N and GNR-PEO2000 self-assembly for drug-resistant bacteria disinfection upon double-light activation. Reprinted with permission from ref 209. Copyright 2020 Wiley-VCH Verlag GmbH & Co. KGaA, Weinheim. (c) NIR light-triggered NO-enhanced PDT and low-temperature PTT-based synergistic approach for biofilm elimination. Reprinted from ref 222. Copyright 2020 American Chemical Society. (d) Double-light-driven therapy of wound infection. Reprinted from ref 225. Copyright 2019 Wiley-VCH Verlag GmbH & Co. KGaA, Weinheim.

treatment area; hypoxia condition could be further induced to hasten the bioreductive drug activities.^{186,187} By co-loading antibacterial drugs and PS into a single nanoparticle, chemotherapy and PDT can concurrently contribute to the highly productive treatment.¹⁸⁸

For example, Wei *et al.* developed a multifunctional nanodevice for the comprehensive treatment of biofilm with TiO₂-coated UCNP and D-amino acid surface. UCNPs core converted NIR light to UV light which stimulate TiO₂ shell to produce ROS and to spatiotemporally release free D-amino acids (D-Tyr) to eradicate bacteria.¹⁸⁹ Chen and co-workers constructed a pH-responsive zeolitic imidazolate framework-8-poly(acrylic acid) (ZIF-8-PAA) material for drug delivery and PS ammonium methylbenzene blue delivery to the bacteria-infected lesion. Roughly, the secondary modification with AgNO₃ and vancomycin/NH₂-poly(ethylene glycol) (Van/NH₂-PEG) was achieved with decent pH responsiveness and excellent drug loading capacity presented by PAA. The significant results were observed after NIR light treatment in three kinds of bacteria, including *Escherichia coli*, *Staphylococcus aureus*, and methicillin-resistant *S. aureus*, revealing a superior therapeutic PDT/AgNPs strategy.¹⁹⁰

To enhance the drug delivery and localized PDT effects, polymer-based photodynamic nanoassembly chitosan-chlorin e6 (Ce6) was conjugated by Zhang's group to exhibit a strong interaction with bacteria, altering the bacteria structure and effectively delivering PS Ce6 into the infectious area.¹⁹¹ Moreover, it is notable that, in the bacterial infection site, HAase is ubiquitously overexpressed, suggesting a strategy for microenvironment-responsive fabrication of nanodevices. In this viewpoint, photosensitive PCN-224 nMOF loaded with Ag ions was coated with HA by Zhang *et al.* After the degradation of HA activated by HAase, the positive charge from an initially neutral nanosystem was exposed to facilitate the specific bacteria

membrane association, showing an outstanding antibacterial result (Figure 5a).¹⁹²

4.7. PDT–PTT. Since PDT relies on intracellular induction of ROS, the enhancement of PS delivery is therefore vital for efficient photodynamic treatment. Interestingly, the uptake of the PDT PS can be improved by increasing the temperature by PTT in the targeted infection area.^{193,194} As well, an increase in temperature by PTT will also effectively accelerate the blood flow with an uplifted vascular O₂ level which consequently benefits PDT by elevating the ¹O₂ yield.^{195,196} Therefore, inducing dual stresses of heat and ROS opens a new opportunity to effectually exterminate bacteria with minimum surrounding tissue damage through lowering the laser intensity and maximizing the treatment condition.^{197–208}

Yu *et al.* developed a supramolecular self-assembled nanocomposite offering dual PDT/PTT activity with broad-spectrum eradication of drug-resistant bacteria. In the introduced system, unique one-dimensional wire-like graphene nanoribbons (GNRs) were coated with a cationic porphyrin (Pp4N) to afford significant ROS production and temperature promotion upon 660 and 808 nm light irradiations. This photostable synergistic system provides excellent antimicrobial effects for complete annihilation in mouse model of dorsal infection (Figure 5b).²⁰⁹ Likewise, Liang's group co-doped a photothermal conjugated polymer with triphenylamine derivative photodynamic agents *via* self-assembling for dual-functional antimicrobial activity with more than 70%, 90%, and 99% killing efficacy for Gram-(−) bacteria (*E. coli*), Gram-(+) bacteria (*S. aureus*), and fungi (*Candida albicans* (*C. albicans*)) under 808 nm light radiation, respectively.²¹⁰

For a polymer with a narrow band gap in the NIR range, a donor–acceptor–donor (D–A–D) structure comprising two electron-rich donors and one electron-deficient acceptor is usually designed as the conjugated backbones. Applying the

construction, synergetic local hyperthermia and ROS eradication of bacteria were observed under 808 nm radiation with valuable fluorescence tracking.²¹¹ Alternatively, the hybrid hydrogel with an enhanced NIR-stimulated PDT effect from the combination of polyisocyanide (PIC) hydrogel, cationic conjugated polythiophene (PMNT), and CPNs-Tat was introduced by Cui and colleagues for germicidal treatment.²¹² Besides organic polymer, a small protein with significant photothermal induction can also be recruited for prospective biocompatible nanosystems.²¹³

Upconversion nanoparticles were applied as NIR-induced mediators for the photodynamic effects upon the activation of delivered PSs. In previous research, a multifunctional upconversion platform for synergistic PDT/PTT antibacterial-resistant therapy was achieved by loading phenothiazinium PS methylene blue (MB) into UCNPs/CuS hybrid. Compared to PDT or PTT alone, the combination therapy realized significant enhancement upon single CW laser irradiation.²¹⁴ In order to minimize the normal tissue injury, highly sensitive PSs excited by lower power density are required. Following this perspective, poly(selenoviologen) was self-assembled on the surface of a core-shell NaYF₄: Yb/Tm@NaYF₄ UCNP exploiting a mild irradiation condition ($\lambda = 980$ nm, 150 mW·cm⁻², and 4 min) for MRSA ablation. The practical phototherapeutic efficiency was attained from strong ROS production and high photothermal conversion efficiency (52.5%) under low-power 980 nm laser illumination.²¹⁵

The formation of ROS in the PDT system is generally being inhibited due to the hypoxic condition under a bacterial-infected wound site. Therefore, oxygen supplying or alteration of ROS generation strategies is pivotal for the development of photodynamic-based antibacterial practices. Innovatively, a light-activated alkyl free radical initiator encapsulated in a polydopamine-coated carboxyl graphene (PDA@CG) was synthesized to produce an excellent infection-responsive antibacterial effect by generating alkyl radicals (R) under various oxygen tension condition. Significant bacterial DNA-damaging activity *in vivo* further showed the extraordinary synergistic therapeutic effect of PDT and PDT under complex physiological environment.²¹⁶

For enhanced *loci* targeting, Zhou *et al.* proposed a positively charged conjugated polymer (PTDBD) with dual photothermal and photodynamic ability for specific targeting and killing of bacteria under relatively mild treatment conditions (40 μ g·mL⁻¹, 1.0 W·cm⁻²).²¹⁷ Hou *et al.* recently exploited the bacterial lectins interaction of galactose in glycosylated plasmonic copper sulfide nanocrystals (Cu_{2-x}S NCs) to specifically ablate *P. aeruginosa* under NIR-II light illumination with simultaneous effects of PTT/PDT.²¹⁸

4.8. PDT-PTT-CHEMO. While the above-mentioned bimodal synergistic antimicrobial treatment exhibited higher efficiency than the monomodal therapy, the efficacy can be further enhanced by trimodal therapy built on cooperation among three therapeutic agents within a single nanosystem. The integration of drug, PSs, and photothermal agents realizes the combination of chemotherapy, PDT, and PTT against bacterial infection with minimum administration dose and lower invasiveness. In these collaborating nanoplatforms, the heat generated from the photothermal agents will increase the uptake of both antimicrobial chemoagents and PSs and amplify the O₂ supply for efficient ROS production. Antibacterial treatment relying on a trifunctional nanostructure that involves various

bacterial killing mechanisms is therefore expected to give a much stronger multimodal bactericidal outcome.²¹⁹⁻²²¹

Trifunctional photothermal-, photodynamic-, and chemotherapy was achieved by the construction of dual-valent platinum nanoparticles (dvPtNPs) composed of Pt⁰ and Pt²⁺ ions by Deng and co-workers. Laser excitation at 808 nm initiated the photothermal destabilization with the release of Pt²⁺ ions as the chemodrug, coexisting with the ROS production for synergistic bacterial ablation.²¹⁹ Similarly, synergistic ablation could be realized by PB@PDA@Ag nanoparticle, disrupting the plasma integrity, generating ROS, reducing ATP, and oxidizing GSH. This nanosystem also showed accelerated MRSA-infected diabetic wound healing indicated by the upregulation of VEGF expression.²²⁰ Furthermore, an all in one phototherapeutics antimicrobial nanoplatform was illustrated in the AI-MPDA nanoparticle by Yuan and co-workers. Complementarily, indocyanine green (ICG) and L-arginine (L-Arg) were encapsulated in mesoporous polydopamine (MPDA) to form AI-MPDA nanoparticles *via* π - π interaction and adsorption. PDT was efficiently generated under mild temperature increase (45 °C) for activation of L-Arg for NO gas production. The NO-enhanced PDT&PTT approach was then performed to damage the bacterial membrane, turning on a robust eradication of biofilm (around 100% in an abscess formation model). Such low dose (0.2 mg·mL⁻¹ of AI-MPDA nanoparticles) and mild temperature treatment condition are significantly less harmful to the surrounding normal tissues and ideal for clinical application of already-formed biofilm (Figure 5c).²²²

Similarly, another PDA-based nanosystem with significant photothermal conversion efficiency was designed for synergistic abolition of MDR bacteria in the diabetic mouse model by Tong and colleagues. PDA-coated PB nanoparticles acted as the scaffold for AgNPs reduction, which indicated a significant elimination of bacteria through cooperative pathways consisting of cell membrane disintegration, ROS elevation, ATP decreasing, and metabolism disruption. Importantly, the nanocomplex functioned as a reduced inflammation platform in the wound area after synergistic therapy, showing a high potential for the treatment of chronic infectious wounds.²²⁰ Dual-functional bacterial removing and wound healing also can be achieved by combining Zn²⁺-doped sheet-like C₃N₄ with GO under a short time exposure to 660 and 808 nm light irradiations.²²³ Meanwhile, the heterojunction of this Zn²⁺-doped C₃N₄ with Bi₂S₃ was fabricated by Li and co-workers with the combination of β -lactam antibiotics to offer an efficient anti-infectious outcome with wound healing promotion, eliminating observable resistances.²²⁴

Specific capture and elimination of bacteria may be obtained by simply modifying the nanoparticle surface with targeting moieties. To further enhance the therapeutic outcomes of synergistic treatment, glycoligands are popularly added to the nanosystem. For example, Hu *et al.* developed a unique glycosheet by galactose- and fructose-based ligands which self-assembled on the surface of thin-layer molybdenum disulfide. Multivalent carbohydrate-lectin interactions promoted the bacterial targeting to precisely kill the bacteria in a combination manner with control-released antibiotic activities, PDT and PTT upon white and NIR light irradiations (Figure 5d).²²⁵

Evidently, some possible shortages of synergistic therapy are still waiting to be avoided by further research. For instance, the complex conjugated nanostructure may generate some biofunctional issues such as not biodegradable and cytotoxicity. The

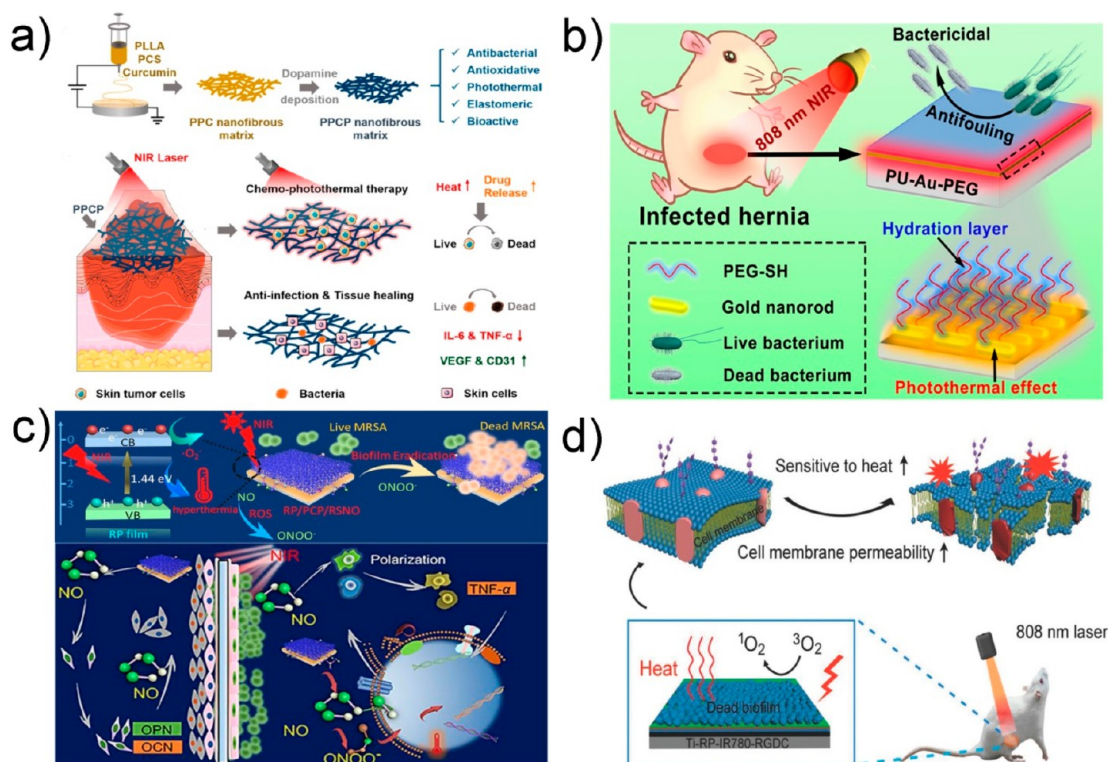


Figure 6. (a) Chemo-photothermal therapy by PPCP nanofibrous scaffolds. Reprinted with permission from ref 237. Copyright 2020 American Chemical Society. (b) Schematic illustration of NIR-responsive PU-Au-PEG surface for antifouling and bacteria killing. Reprinted with permission from ref 238. Copyright 2020 American Chemical Society. (c) Schematic diagram of NIR light-triggered biofilm eradication and the mechanisms of promoted bone formation. Reprinted with permission from ref 256. Copyright 2020 American Chemical Society. (d) Schematic illustration of the disinfection of the bacteria on the bone implant upon 808 nm laser irradiation. Reprinted with permission from ref 258. Copyright 2018 Wiley-VCH Verlag GmbH & Co. KGaA, Weinheim.

simplicity of design can be achieved by innovation of a single type of material bearing the ability with multiple synergistic treatment effects. In addition, more targeting moieties need to be further investigated in the *ex vivo* tissue or *in vivo* infected area to realize the maximum effective targeting in a lesion. The metabolic labeling method may be a promising candidate to solve this problem.

5. BACTERIAL DISINFECTION BEYOND NANOPARTICLES

Because the above discussion mainly revolved around the NIR-responsive antibacterial nanoparticle, we are going to focus on the various antimicrobial approaches beyond the nanoparticle, which include antibacterial film, antibacterial implantation, and hydrogel application.

5.1. Antibacterial Film. The film material possesses unique properties originating from its flexibility/stretchability, great pore interconnectivity, and specific physicochemical properties, allowing it to be sturdily developed in diverse applications such as water cleaning systems, energy storage devices, and antibacterial platforms, *etc.*^{226,227} In particular, some of the characteristics are rendering films to not only effectively shield acute or chronic wounds from pathogens and dehydration but also intrinsically promote hemostasis and tissue regeneration for wound healing, which endow the film material to be a promising candidate for curing microbial infections.^{228–236} Additionally, NIR-excitable film coating is frequently designed to eradicate biofilms or planktonic bacteria colonized on the device surface in deep-tissue treatment. In this segment, we will elaborately

discuss the recent design of NIR-associated films for bacterial disinfection.

For example, Li and co-workers introduced a biodegradable ultralong copper sulfide nanowire-reinforced poly(citrate-siloxane) nanocomposites elastomer, exhibiting modulatable mechanical elasticity, tunable electronic conductivity, strong NIR photothermal capacity, and broad-spectrum antibacterial activity, with its remarkable real-time thermal-imaging feature *in vivo*.²³¹ Xi *et al.* designed a multifunctional elastomeric poly(L-lactic acid)-poly(citrate siloxane)-curcumin @ polydopamine hybrid nanofibrous scaffold for simultaneous tumor ablation, antibacterial infection, and wound healing. After the photothermal extirpation of bacteria by NIR light, the nanofibrous matrix concurrently up-regulated the VEGF and the cluster of differentiation 31 (CD31) immunorexpression in the endothelial cells, which play pivotal roles in the early angiogenesis, thus promoting the adhesion and proliferation of normal skin cells in bacterial-infected mice (Figure 6a).²³⁷ To overcome the biomedical device-associated infection, Zhao *et al.* introduced an NIR-responsive organic/inorganic polyurethane (PU) hybrid which functionalized with photothermal Au nanorod and antifouling PEG, averting the hydrophobic interaction between bacteria and prosthetic mesh PU for the subcutaneous hernia repair. This platform could not only effectively ablate pathogen bacteria including MDR bacteria *in vivo* upon 808 nm NIR irradiation but also successfully prevent accumulation of bacterial debris without the external stimuli because of its antifouling property (Figure 6b).²³⁸ In consideration of the platform regenerability, Budimir *et al.* created a Kapton/Au nanoholes substrate coated with rGO-PEI thin films with

excellent reusability to destroy the *S. epidermidis* biofilm.²³⁹ Kim and co-workers engineered an antibacterial microreactor by using catechol-grafted poly(*N*-vinylpyrrolidone) and immobilization of NIR-active $\text{Cs}_{0.33}\text{WO}_3$ nanoparticles inside the poly(dimethylsiloxane) (PDMS)-based microreactors. The continuous flow and adhesion of bacteria could be eradicated by NIR light-induced photothermal reaction, and the mussel-inspired immobilized $\text{Cs}_{0.33}\text{WO}_3$ nanoparticles could easily be cleaned by simple acid treatment for a recyclable microreactor.²⁴⁰ Moreover, Qu and co-workers fabricated diverse substrates by sequential deposition of a gold nanoparticle layer and a phase-transitioned lysozyme film (PTLF). The photothermal effect from the Au layer induced by NIR laser could kill 99% of attached bacteria in 5 min with recyclable PTLF surface by immersion in Vitamin C.²⁴¹ The previous examples necessitate the degradation of the platform layer for surface regeneration upon every new usage. To boost the ease of use, Wang *et al.* reported a smart antibacterial hybrid film based on tannic acid/ Fe^{3+} ion (TA/ Fe) complex and PNIPAM. The immobilized PNIPAM intriguingly possesses the heat-triggered fouling-repellent ability, which is capable of removing dead bacteria and other debris at 4 °C.²⁴²

5.2. Antibacterial Implantation. Bioimplantations and devices were prominently developed for soreness alleviation and function revitalization to improve the quality of life. Nevertheless, these implants were often subjected to bacterial infection, increasing the patient morbidity and mortality. In other words, the bioimplants are vulnerable to infections across nearly all bioapplications, such as the internal articular prosthetics,²⁴³ the implantable cardiovascular devices,²⁴⁴ the abdominal wall implants, or even the external carriers such as contact lenses.^{245,246} To prevent implant-associated infection, efforts have been recognized on the basis of several strategies such as adhesion resistance, contact killing, and biocide leaching.²⁴⁷ However, there are existing issues in accordance to these strategies: (i) adhesion resistance approach often prevents bacteria adhesion; however, the planktonic microbes are still suspended in the body. (ii) Contact killing, which is described as surface-adhered bacterial cell lysis, frequently uses pH-responsive antimicrobial peptides and is susceptible to proteolysis, suggesting lower antibacterial efficacy. (iii) Biocide leaching, which utilizes heavy metal ions and antibiotics, often introduces cytotoxicity to surrounding normal healthy tissues and builds up the severe antibiotic resistance of bacteria, respectively. To overcome these setbacks, materials that were previously discovered were applied for antiseptic implantation accompanied by advanced technologies such as photothermal, photodynamic, and synergistic therapies.^{248–250} This review section exemplifies some of the work done in different advanced therapy systems including several synergistic implant-associated infection therapies.

In an individual PDT system, Tan and co-workers constructed the surface of the frequently used biocompatible metal implant, titanium metal, with liposome encapsulated PS IR780, and perfluorohexane to yield high antibacterial efficacy.²⁵¹ Moreover, in a PTT system, Zhang and co-workers discovered rhenium trioxide (ReO_3) as a commendable photothermal nanoplatform. This platform also allows photoacoustic imaging and CT imaging, potentiating the multimodal imaging-guided diagnosis and therapy for implant-related infections.²⁵² Furthermore, Zhao *et al.* reported a titanium metal decorated with zinc oxide@collagen type I which is dual-light-excitatable for specific corresponding activation. The antibacterial effect of

ZnO was activated by 583 nm yellow light, whereas the osseointegration was accelerated by heating effect under 808 nm NIR excitation.²⁵³ Correspondingly, to promote effective osteogenesis and efficient photoresponsive antibacterial effect, Deng and co-workers fabricated a multifunctional orthopedic material consisting of sulfonated poly(ether-ether-ketone) conjugated graphene oxide nanosheets, PDA, and adiponectin protein to facilitate *in vivo* bone formation. Intriguingly, this platform could not only accelerate the new bone formation but also perform as a recyclable antimicrobial platform, especially suitable for biomaterial-associated repeated infection.²⁵⁴

To illustrate the various synergistic bacterial therapies, a NIR-induced PTT/silver ions platform was adopted by Wang and co-workers by hybridizing the chitosan, silver nanoparticles, and MnO_2 nanosheets onto the surface of titanium metal as coating. Since chitosan composite greatly stabilized the Ag nanoparticle, the slow release of Ag^+ ions could trigger the conversion of oxidation stress indicator, GSH to GSSG, inducing bacterial membrane damage and its vulnerability.²⁵⁵ Moreover, PTT could be coupled with immunotherapy to eliminate methicillin-resistant *S. aureus* biofilm infection on bone implant as reported by Li *et al.* Along with photothermal effect, NO release, and $^{\cdot}\text{OONO}$ formation, the immunotherapy by NO-induced M1 macrophage polarization was confirmed through the upregulation of the TNF- α and IL-6 expression, indicating the tissue regeneration effect of NO (Figure 6c).²⁵⁶

In a synergistic PDT/PTT system, Feng and co-workers covalently grafted the surface of titanium with chitosan-modified molybdenum sulfide nanosheets for dual-light-activation (660 nm visible light for singlet oxygen generation, 808 nm NIR light for hyperthermia induction) synergistic PDT/PTT therapy. Although bacterial eradication efficiency was optimally achieved, the process is rather onerous to incorporate two-light activation to ablate bacterial cells.²⁵⁷ This research group further enhanced their antibacterial implant application with single NIR light activation. Similarly, on the titanium alloy, they decorated it with photothermal-responsive red phosphorus/PDA, singlet oxygen generating IR780 dye and an arginine-glycine-aspartic acid-cysteine short peptide for improved bacterial cell adhesion and accelerated bone tissue regeneration (Figure 6d).²⁵⁸ Besides, Hong and co-workers offered a system by incorporating bismuth sulfide inorganic semiconductor as the stable ROS generator rather than exploiting iodide dye which suffers from poor stability. Bismuth sulfide combined with trisilver phosphate was conjugated on titanium metal to achieve high photocatalytic performance and higher ROS yield for synergistic biofilm elimination.²⁵⁹ Furthermore, Yuan *et al.* introduced a modification of MPDA nanoparticles that loaded with ICGs as the photosensitizer and RGDs as the osteogenic peptide onto a titanium implant to trigger ROS for bacterial membrane destruction upon 808 nm laser excitation. It likewise demonstrated excellent osseointegration between living bone and implants, as well as osteogenesis effect proved by the positive growth of mesenchymal stem cells.²⁶⁰

5.3. Hydrogel. Hydrogels have emerged as one of the most significant design breakthroughs for the manipulation of dynamic molecular interactions. Hydrogels have evolved from simple physically or chemically cross-linked structures to composite engineered materials that can potentiate native cell functions or ablate tumor/bacterial cells in various applications, such as drug delivery platforms, nanoparticle decorative moieties, and so on.^{261,262} Smart hydrogels, which are particularly sensitive to physical and chemical stimuli such as

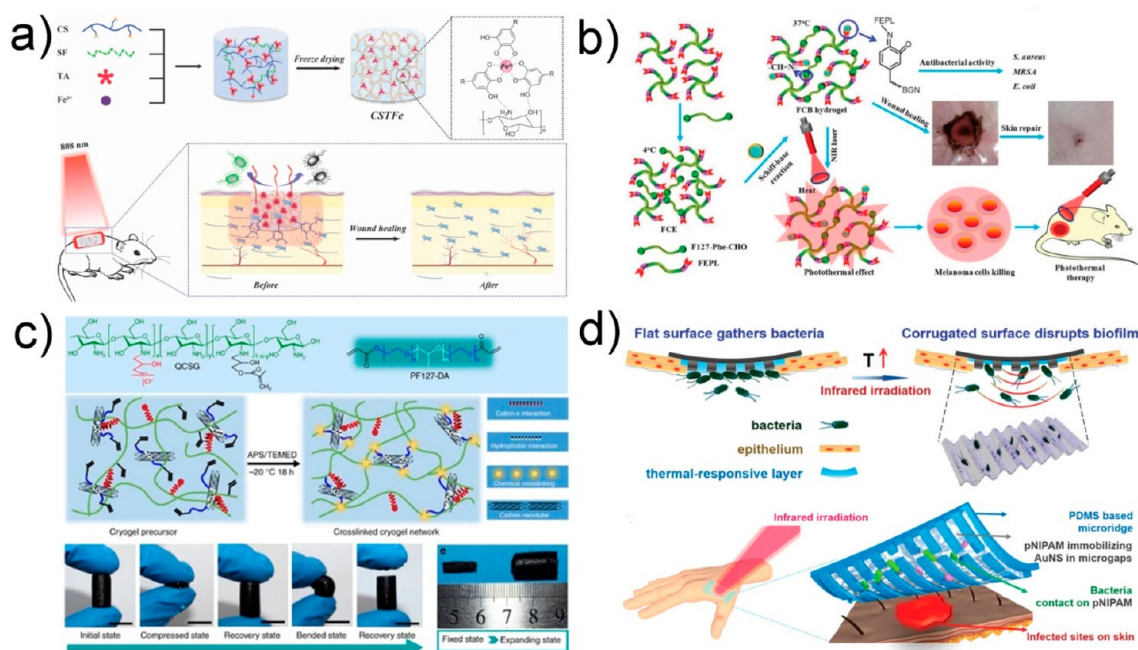


Figure 7. (a) NIR light-responsive cryogels as wound dressing materials. Reprinted with permission from ref 275. Copyright 2019 Wiley-VCH Verlag GmbH & Co. KGaA, Weinheim. (b) Scheme illustration of the FCB hydrogel for tumor therapy and wound healing. Reprinted with permission from ref 277. Copyright 2019 Wiley-VCH Verlag GmbH & Co. KGaA, Weinheim. (c) Structure of QCSG/CNT cryogel. Reprinted with permission from ref 280. Copyright 2018 The Author(s) under Creative Commons Attribution 4.0 International License (<https://creativecommons.org/licenses/by/4.0/>). (d) TRIM films for photothermal elimination of various bacteria. Reprinted with permission from ref 281. Copyright 2020 Wiley-VCH Verlag GmbH & Co. KGaA, Weinheim.

photon excitation, temperature, electrostatic interaction, pH, and cognitive ions or molecules, have been adopted for a variety of research designs.²⁶³ Because of their broad range of stimuli-responsive functionalities, hydrogels' structural properties have been prevalently refined and incorporated into NIR photothermal design strategies for specific bacterial targeting and ablation effects.^{264–269} Recently, the use of mussel-inspired chemistry in forming hydrogels has been widely explored for bioapplications, electronics, and soft robotics, *etc.* Generally, three main building blocks, polyphenols, polydopamine, and catechol-based polymers, have been well-developed for hydrogel formation.²⁷⁰ This review section discusses the implementation of hydrogels in NIR-based photothermal bacterial elimination, which associated with effective wound dressing ability, in accordance with the hydrogels' modification with various emerging materials and their general bonding characteristics, for instance, covalent and noncovalent bond formation based on the building block linkage.

Noncovalent interactions comprise hydrogen bonding, hydrophobic interactions, and π - π interactions. For example, an antimonene sheet could coat with bacteria-targeting network polymer holding great potential in NIR-assisted photothermal bacteria eradication and wound healing.²⁶⁶ Furthermore, Hsiao and co-workers designed a smart pH-responsive hydrogel formed by the conjugation of chitosan with mercaptopropyl sulfonic acid (MPS)-modified PANI for localized photothermal bacterial treatment. Chitosan, acting as a hydrogen donor/acceptor, plays a crucial role in pH-responsive hydrogelation, while self-doped MPS-modified polyaniline is a compatible conducting polymer. In an inflamed abscess at pH 6.0–6.6, the hydrogel was in an injectable aqueous form, whereas the hydrogel-formed colloids at pH 7.0–7.4, preventing targeting in normal healthy tissue. Excitation by an 808 nm laser at 2.0 W·

cm⁻² subsequently ablates the pathogenic bacteria concentrated with the hydrogels.²⁷¹ Mohamed *et al.* constructed plasmonic Au nanoparticles conjugated with poly(*N*-vinylcaprolactam) (PVCL) to form a smart hydrogel responsive to temperature. The PVCL nanorod exhibits a lower critical solution temperature (LCST) of 35 °C, where polymer dissolution occurs at low temperature, resulting in liquid form due to hydrogen bonding with water; temperatures above the LCST initiate the decomposition of hydrogen bonding, and the formation of hydrophobic interactions dominates upon exposure to a 785 nm diode laser, resulting in a phase change from solution to gel form for efficient targeted bacterial ablation.²⁷² Adopting a similar thermally controlled solution–gel strategy, Ko and co-workers developed an effective photothermal nanocomposite composed of poly(3,4-ethylenedioxythiophene):poly(styrene-sulfonate) (PEDOT:PSS) and agarose, achieving a sharp temperature increase upon NIR exposure for light-excited self-healing ability and antibacterial effects.²⁷³ Wang and co-workers introduced pH-responsive supramolecular nanofiber networks by the self-assembly of Ac-Leu-Lys-Phe-Gln-Phe-His-Phe-Asp-NH₂ (IKFQFHFD) octapeptide loaded with cypate as a photothermal agent and proline as a procollagen component for healing purposes. The biocompatible octapeptide self-assembles at neutral pH due to the side chains of phenylalanine amino acids potentiating intermolecular π - π stacking. Hydrogel self-assembly is also dictated by the intermolecular ionic interaction and the hydrogen bonding formed between peptide molecules. Upon a pH change from neutral to acidic pH, the supramolecular hydrogel could perform on-demand cypate and proline release to promote photothermal killing and cell proliferation processes for wound healing, respectively.²⁷⁴

Because of the development of hydrogels with covalent interactions, metal-chelated phenolic compounds and Schiff-

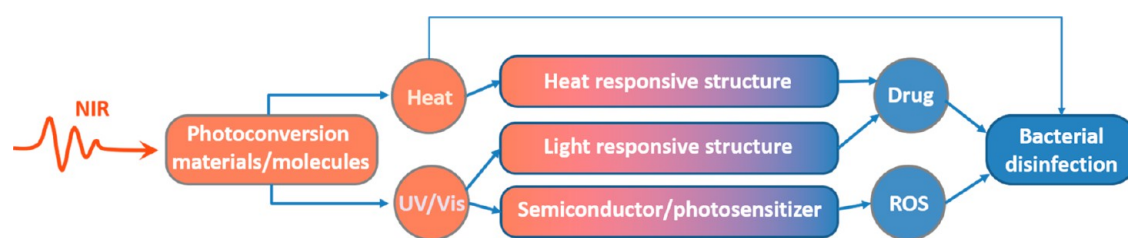


Figure 8. Schematic illustration of the mechanism of NIR light-based bacterial disinfection.

based formation have been widely adopted for NIR photothermal-responsive hydrogels. Yu *et al.* fabricated a photothermal-responsive cryogel composed of chitosan/silk fibroin as a scaffold and tannic acid/ferric ions (TA/Fe³⁺) as the photoresponsive thermal agent (CSTFe). Covalent metal-phenolic chelation interaction between the tannic acid and ferric ion was employed as the photothermally responsive moiety. Intermolecular hydrogen bonding between the chitosan and TA/Fe³⁺ maintained the cryogel structure. The metal-chelated TA/Fe³⁺ complex was important in both the 808 nm-laser-irradiated photothermal bacteria killing and the wound healing process, as described. The as-synthesized cryogel underwent hemostasis evaluation and was shown to possess good blood absorption and blood clotting properties, making it a potent hemostasis material (Figure 7a).²⁷⁵ Similarly, Deng and co-workers suggest the use of TA/Fe³⁺ in the formation of agarose-based hydrogel composites for complementary NIR treatment.²⁷⁶ Exploiting kindred wound healing and antibacterial photothermal hydrogels, Zhou and co-workers formulated a polypeptide-based hybrid nanosystem by cofunctionalizing the PDA building blocks and F127-pretreated EPL polypeptide (FEPL). The hydrogel was formed through Schiff-base covalent interaction between the PDA and the amino group of FEPL, which possess the functions of photothermal induction and antimicrobial ability, respectively. It was proven that the bioactive glass-PDA conjugated with FEPL decreased the wound area to 8.3%, in distinct contrast with the 31.8% result in the control group, thus establishing excellent wound healing ability (Figure 7b).²⁷⁷ Furthermore, Zhao and co-workers utilized the catechol-Fe³⁺ complex for pH responsiveness as well as the antioxidant ability of catechol to scavenge the overproduction of ROS for improved wound healing processes, which has rarely been reported.²⁷⁸

Different types of emerging photothermal frameworks and biodevices have also been revealed. For instance, thermal ablation of bacteria was achieved by the charge transfer between ferrous ions and ferric ions in the PB MOF structure triggered by NIR photons, while the bacterial capture realized by the hydrogel electrostatic attraction allowing tight absorption between the framework and the surface potential of bacteria, inducing an effective bacterial elimination.²⁷⁹ In addition, Zhao and co-workers obtained cryogel with good mechanical strength and NIR-stimuli responsiveness by incorporating CNTs. They invented an injectable shape memory hemostatic dressing consisting of CNT-reinforced antibacterial conductive nanocomposite cryogels that could realize excellent hemostatic effects compared to plain cryogels without CNT conjugation in a mouse liver injury model, mouse-tail amputation model, rabbit liver defect lethal noncompressible hemorrhage model, and standardized circular liver bleeding model (Figure 7c).²⁸⁰ Intriguingly, Hu *et al.* reported a novel localized thermal management strategy termed thermal-disrupting interface-

induced mitigation (TRIM) to establish a topical antibacterial therapy with negligible cohesion loss of epidermal tissue during the thermoablation process. They incorporated PDMS-based flexible substrate size-controlled TRIM integrating a biomimetic topography of 3 μm, as larger topography leads to unwanted biofilm formation that hinders bacterial killing. This TRIM film accommodated the dispersed localization of bacteria, and subsequently, a modest intensity of NIR photoactivation at 70 mW·cm⁻² triggered the shrinking of the PNIPAM hydrogel and localized the Au nanostars in the microvalleys of the film, concentrating the photothermal agents near the bacteria for photothermal ablation (Figure 7d).²⁸¹

6. CONCLUSION

In summary, by utilizing the light-responsive materials and molecules as mediators, the energy of NIR light could be converted for heat generation, ROS generation, and drug release (Figure 8), which respectively are responsible for photothermal therapy, photodynamic therapy, and synergistic therapy. These therapy systems based on NIR-light response have been widely applied in antibacterial studies, such as those involving wound healing, tissue infection treatment, and inflammation clearance. Though NIR-mediated materials have exhibited promising antibacterial effects and enlightened broader audiences in a medical perspective, the clinical application of a NIR-assisted therapy system still requires many efforts. For instance, since biosafety of NIR light-responsive materials is undoubtedly the primary problem encountered by the clinical application, the development of new and potent NIR molecules or materials with long-term biocompatibility and promising light converting efficacy suitable for clinical translation still demands more science and engineering interventions. In addition, the safety of laser irradiation is also of concern, especially the high-power and long-duration laser irradiation that may pose possible adverse effects to normal tissue. Thus, personalized, low-cost, and reliable therapeutic laser devices that can ideally achieve effective NIR light-mediated inactivation of bacteria, especially MDR strains of bacteria, are highly desirable for the well-being of patients. In short, two significant criteria including the smallest possible dosage of therapeutic agents and the optimal laser irradiation power and time should be thoroughly contemplated to obtain the potent therapeutic effect and at the same time to circumvent various side effects. These deliberations should be taken into account prior to the implementation of NIR nanodrugs in clinical treatments. In addition, to achieve safe and efficient treatment, the designing of a precision treatment system is undeniably the best approach. For NIR-assisted therapy, an optimized therapy should include three precisions, namely, precise medication, precise irradiation area, and precise irradiation time. To achieve these three precisions, the NIR therapeutic system is suggested to be designed according to the following aspects:

- (1) Enhance the bacterial targeting capability. By modifying with antibodies, aptamers, and targeted peptides to enhance the bacteria recognition ability of nanodrugs, accurate delivery can be achieved, so as to effectively reduce the dosage of nanodrugs and reduce the side effects on normal tissues.
- (2) Design the responsive therapeutic system. By combining treatment with a bacteria-detection imaging platform, the visualization of bacteria can be realized and precision irradiation treatment can be guided.
- (3) Construct the therapeutic-effect feedback platform. By integrating the bacterial treatment system with heat, free radical, and bacterial endotoxin, probes could be attained to acquire the therapeutic effect in time and to realize the precise implementation of irradiation time on demand.

AUTHOR INFORMATION

Corresponding Authors

Zhijun Zhang – Department of Chemistry, Zhejiang Sci-Tech University, Hangzhou 310018, China; orcid.org/0000-0002-5470-9491; Email: zjzhang@zstu.edu.cn

Bengang Xing – Division of Chemistry and Biological Chemistry, School of Physical & Mathematical Sciences and School of Chemical and Biomedical Engineering, Nanyang Technological University, Singapore 637371, Singapore; orcid.org/0000-0002-8391-1234; Email: bengang@ntu.edu.sg

Authors

Qinyu Han – Division of Chemistry and Biological Chemistry, School of Physical & Mathematical Sciences, Nanyang Technological University, Singapore 637371, Singapore

Jun Wei Lau – Division of Chemistry and Biological Chemistry, School of Physical & Mathematical Sciences, Nanyang Technological University, Singapore 637371, Singapore

Thang Cong Do – Division of Chemistry and Biological Chemistry, School of Physical & Mathematical Sciences, Nanyang Technological University, Singapore 637371, Singapore

Complete contact information is available at:
<https://pubs.acs.org/10.1021/acsabm.0c01341>

Notes

The authors declare no competing financial interest.

ACKNOWLEDGMENTS

Z.Z. acknowledges the financial support from the National Natural Science Foundation of China (NSFC; Grant No. 22007083), the Zhejiang Provincial Natural Science Foundation of China (Grant No. LQ20B010010), and the Science Foundation of Zhejiang Sci-Tech University (ZSTU) under Grant No. 19062410-Y. B.X. acknowledges the financial support from Tier 1 RG5/18 (S), RG6/20, and MOE 2017-T2-2-110, a Start-Up Grant (SUG), A*Star SERC Grant Nos. A1983c0028 (M4070319) and A20E5c0090, and the NSFC (Grant No. 51929201).

REFERENCES

- (1) Langford, B. J.; So, M.; Raybardhan, S.; Leung, V.; Westwood, D.; MacFadden, D. R.; Soucy, J.-P. R.; Daneman, N. Bacterial co-infection and secondary infection in patients with COVID-19: a living rapid review and meta-analysis. *Clin. Microbiol. Infect.* **2020**, *26*, 1622–1629.
- (2) Zumla, A.; Nahid, P.; Cole, S. T. Advances in the development of new tuberculosis drugs and treatment regimens. *Nat. Rev. Drug Discovery* **2013**, *12*, 388–404.
- (3) Tagliabue, A.; Rappuoli, R. Changing Priorities in Vaccinology: Antibiotic Resistance Moving to the Top. *Front. Immunol.* **2018**, *9*, 1068–1068.
- (4) Lewis, K. Platforms for antibiotic discovery. *Nat. Rev. Drug Discovery* **2013**, *12*, 371–387.
- (5) Linklater, D. P.; Baulin, V. A.; Juodkakis, S.; Crawford, R. J.; Stoodley, P.; Ivanova, E. P., Mechano-bactericidal actions of nanostructured surfaces. *Nat. Rev. Microbiol.* **2020**, DOI: [10.1038/s41579-020-0414-z](https://doi.org/10.1038/s41579-020-0414-z).
- (6) Zhang, Z.; Li, M.; Ren, J.; Qu, X. Cell-Imprinted Antimicrobial Bionanomaterials with Tolerable Toxic Side Effects. *Small* **2015**, *11*, 1258–1264.
- (7) Zhang, Z.; Guan, Y.; Li, M.; Zhao, A.; Ren, J.; Qu, X. Highly stable and reusable imprinted artificial antibody used for in situ detection and disinfection of pathogens. *Chem. Sci.* **2015**, *6*, 2822–2826.
- (8) Velema, W. A.; van der Berg, J. P.; Hansen, M. J.; Szymanski, W.; Driessen, A. J. M.; Feringa, B. L. Optical control of antibacterial activity. *Nat. Chem.* **2013**, *5*, 924–928.
- (9) Makabenta, J. M. V.; Nabawy, A.; Li, C.-H.; Schmidt-Malan, S.; Patel, R.; Rotello, V. M., Nanomaterial-based therapeutics for antibiotic-resistant bacterial infections. *Nat. Rev. Microbiol.* **2020**, DOI: [10.1038/s41579-020-0420-1](https://doi.org/10.1038/s41579-020-0420-1).
- (10) Ray, P. C.; Khan, S. A.; Singh, A. K.; Senapati, D.; Fan, Z. Nanomaterials for targeted detection and photothermal killing of bacteria. *Chem. Soc. Rev.* **2012**, *41*, 3193–3209.
- (11) Yang, X.; Yang, J.; Wang, L.; Ran, B.; Jia, Y.; Zhang, L.; Yang, G.; Shao, H.; Jiang, X. Pharmaceutical Intermediate-Modified Gold Nanoparticles: Against Multidrug-Resistant Bacteria and Wound-Healing Application via an Electrospun Scaffold. *ACS Nano* **2017**, *11*, 5737–5745.
- (12) Wei, T.; Yu, Q.; Chen, H. Responsive and Synergistic Antibacterial Coatings: Fighting against Bacteria in a Smart and Effective Way. *Adv. Healthcare Mater.* **2019**, *8*, 1801381.
- (13) Yang, J.; Wang, C.; Liu, X.; Yin, Y.; Ma, Y.-H.; Gao, Y.; Wang, Y.; Lu, Z.; Song, Y. Gallium–Carbenicillin Framework Coated Defect-Rich Hollow TiO₂ as a Photocatalyzed Oxidative Stress Amplifier against Complex Infections. *Adv. Funct. Mater.* **2020**, *30*, 2004861.
- (14) Wang, Y.; Yang, Y.; Shi, Y.; Song, H.; Yu, C. Antibiotic-Free Antibacterial Strategies Enabled by Nanomaterials: Progress and Perspectives. *Adv. Mater.* **2020**, *32*, 1904106.
- (15) Makvandi, P.; Wang, C.-y.; Zare, E. N.; Borzacchiello, A.; Niu, L.-n.; Tay, F. R. Metal-Based Nanomaterials in Biomedical Applications: Antimicrobial Activity and Cytotoxicity Aspects. *Adv. Funct. Mater.* **2020**, *30*, 1910021.
- (16) Liu, Y.; Shi, L.; Su, L.; van der Mei, H. C.; Jutte, P. C.; Ren, Y.; Busscher, H. J. Nanotechnology-based antimicrobials and delivery systems for biofilm-infection control. *Chem. Soc. Rev.* **2019**, *48*, 428–446.
- (17) Li, X.; Bai, H.; Yang, Y.; Yoon, J.; Wang, S.; Zhang, X. Supramolecular Antibacterial Materials for Combatting Antibiotic Resistance. *Adv. Mater.* **2018**, No. 31, 1805092.
- (18) Sun, D.; Pang, X.; Cheng, Y.; Ming, J.; Xiang, S.; Zhang, C.; Lv, P.; Chu, C.; Chen, X.; Liu, G.; Zheng, N. Ultrasound-Switchable Nanozyme Augments Sonodynamic Therapy against Multidrug-Resistant Bacterial Infection. *ACS Nano* **2020**, *14*, 2063–2076.
- (19) Pang, X.; Xiao, Q.; Cheng, Y.; Ren, E.; Lian, L.; Zhang, Y.; Gao, H.; Wang, X.; Leung, W.; Chen, X.; Liu, G.; Xu, C. Bacteria-Responsive Nanoliposomes as Smart Sonotheranostics for Multidrug Resistant Bacterial Infections. *ACS Nano* **2019**, *13*, 2427–2438.
- (20) Xu, J.-W.; Yao, K.; Xu, Z.-K. Nanomaterials with a photothermal effect for antibacterial activities: an overview. *Nanoscale* **2019**, *11*, 8680–8691.
- (21) Zou, Y.; Zhang, Y.; Yu, Q.; Chen, H., Photothermal bactericidal surfaces: killing bacteria using light instead of biocides. *Biomater. Sci.* **2020**, DOI: [10.1039/D0BM00617C](https://doi.org/10.1039/D0BM00617C).

- (22) Feng, Y.; Liu, L.; Zhang, J.; Aslan, H.; Dong, M. Photoactive antimicrobial nanomaterials. *J. Mater. Chem. B* **2017**, *5*, 8631–8652.
- (23) Li, W.; Dong, K.; Wang, H.; Zhang, P.; Sang, Y.; Ren, J.; Qu, X. Remote and reversible control of in vivo bacteria clustering by NIR-driven multivalent upconverting nanosystems. *Biomaterials* **2019**, *217*, 119310.
- (24) Dong, K.; Ju, E.; Gao, N.; Wang, Z.; Ren, J.; Qu, X. Synergistic eradication of antibiotic-resistant bacteria based biofilms in vivo using a NIR-sensitive nanoplatform. *Chem. Commun.* **2016**, *52*, 5312–5.
- (25) Sun, H.; Lv, F.; Liu, L.; Gu, Q.; Wang, S. Conjugated Polymer Materials for Photothermal Therapy. *Adv. Ther.* **2018**, *1*, 1800057.
- (26) Wang, Y.; Jin, Y.; Chen, W.; Wang, J.; Chen, H.; Sun, L.; Li, X.; Ji, J.; Yu, Q.; Shen, L.; Wang, B. Construction of nanomaterials with targeting phototherapy properties to inhibit resistant bacteria and biofilm infections. *Chem. Eng. J.* **2019**, *358*, 74–90.
- (27) Yougbaré, S.; Mutalik, C.; Krisnawati, D. I.; Kristanto, H.; Jazidie, A.; Nuh, M.; Cheng, T.-M.; Kuo, T.-R. Nanomaterials for the Photothermal Killing of Bacteria. *Nanomaterials* **2020**, *10*, 1123.
- (28) Chen, H.; Jin, Y.; Wang, J.; Wang, Y.; Jiang, W.; Dai, H.; Pang, S.; Lei, L.; Ji, J.; Wang, B. Design of smart targeted and responsive drug delivery systems with enhanced antibacterial properties. *Nanoscale* **2018**, *10*, 20946–20962.
- (29) Dharmaratne, P.; Sapugahawatte, D. N.; Wang, B.; Chan, C. L.; Lau, K.-M.; Lau, C. B. S.; Fung, K. P.; Ng, D. K. P.; Ip, M. Contemporary approaches and future perspectives of antibacterial photodynamic therapy (aPDT) against methicillin-resistant *Staphylococcus aureus* (MRSA): A systematic review. *Eur. J. Med. Chem.* **2020**, *200*, 112341.
- (30) Jia, Q.; Song, Q.; Li, P.; Huang, W. Rejuvenated Photodynamic Therapy for Bacterial Infections. *Adv. Healthcare Mater.* **2019**, *8*, 1900608.
- (31) Karahan, H. E.; Wiraja, C.; Xu, C.; Wei, J.; Wang, Y.; Wang, L.; Liu, F.; Chen, Y. Graphene Materials in Antimicrobial Nanomedicine: Current Status and Future Perspectives. *Adv. Healthcare Mater.* **2018**, *7*, 1701406.
- (32) Lam, S. J.; Wong, E. H. H.; Boyer, C.; Qiao, G. G. Antimicrobial polymeric nanoparticles. *Prog. Polym. Sci.* **2018**, *76*, 40–64.
- (33) Pang, X.; Li, D.; Zhu, J.; Cheng, J.; Liu, G. Beyond Antibiotics: Photo/Sonodynamic Approaches for Bacterial Theranostics. *Nano-Micro Lett.* **2020**, *12*, 144.
- (34) Zhao, J.; Duan, L.; Wang, A.; Fei, J.; Li, J. Insight into the efficiency of oxygen introduced photodynamic therapy (PDT) and deep PDT against cancers with various assembled nanocarriers. *Wiley Interdiscip. Rev.: Nanomed. Nanobiotechnol.* **2020**, *12*, e1583.
- (35) de Melo-Diogo, D.; Lima-Sousa, R.; Alves, C. G.; Correia, I. J. Graphene family nanomaterials for application in cancer combination photothermal therapy. *Biomater. Sci.* **2019**, *7*, 3534–3551.
- (36) Tou, M.; Luo, Z.; Bai, S.; Liu, F.; Chai, Q.; Li, S.; Li, Z. Sequential coating upconversion NaYF₄:Yb,Tm nanocrystals with SiO₂ and ZnO layers for NIR-driven photocatalytic and antibacterial applications. *Mater. Sci. Eng., C* **2017**, *70*, 1141–1148.
- (37) Li, J.; Zhao, Q.; Shi, F.; Liu, C.; Tang, Y. NIR-Mediated Nanohybrids of Upconversion Nanophosphors and Fluorescent Conjugated Polymers for High-Efficiency Antibacterial Performance Based on Fluorescence Resonance Energy Transfer. *Adv. Healthcare Mater.* **2016**, *5*, 2967–2971.
- (38) Castano, A. P.; Demidova, T. N.; Hamblin, M. R. Mechanisms in photodynamic therapy: part one—photosensitizers, photochemistry and cellular localization. *Photodiagn. Photodyn. Ther.* **2004**, *1*, 279–293.
- (39) Zhou, B.; Shi, B.; Jin, D.; Liu, X. Controlling upconversion nanocrystals for emerging applications. *Nat. Nanotechnol.* **2015**, *10*, 924–936.
- (40) You, W.; Tu, D.; Zheng, W.; Shang, X.; Song, X.; Zhou, S.; Liu, Y.; Li, R.; Chen, X. Large-scale synthesis of uniform lanthanide-doped NaREF₄ upconversion/downshifting nanoprobles for bioapplications. *Nanoscale* **2018**, *10*, 11477–11484.
- (41) Zhang, Z.; Han, Q.; Lau, J. W.; Xing, B. Lanthanide-Doped Upconversion Nanoparticles Meet the Needs for Cutting-Edge Bioapplications: Recent Progress and Perspectives. *ACS Mater. Lett.* **2020**, *2*, 1516–1531.
- (42) Thang, D. C.; Wang, Z.; Lu, X.; Xing, B. Precise cell behaviors manipulation through light-responsive nano-regulators: recent advance and perspective. *Theranostics* **2019**, *9*, 3308–3340.
- (43) Liu, J.; Yu, M.; Zeng, G.; Cao, J.; Wang, Y.; Ding, T.; Yang, X.; Sun, K.; Parvizi, J.; Tian, S. Dual antibacterial behavior of a curcumin–upconversion photodynamic nanosystem for efficient eradication of drug-resistant bacteria in a deep joint infection. *J. Mater. Chem. B* **2018**, *6*, 7854–7861.
- (44) Xu, F.; Hu, M.; Liu, C.; Choi, S. K. Yolk-structured multifunctional up-conversion nanoparticles for synergistic photo-dynamic-sonodynamic antibacterial resistance therapy. *Biomater. Sci.* **2017**, *5*, 678–685.
- (45) Grüner, M. C.; Arai, M. S.; Carreira, M.; Inada, N.; de Camargo, A. S. S. Functionalizing the Mesoporous Silica Shell of Upconversion Nanoparticles To Enhance Bacterial Targeting and Killing via Photosensitizer-Induced Antimicrobial Photodynamic Therapy. *ACS Appl. Bio Mater.* **2018**, *1*, 1028–1036.
- (46) Xu, F.; Zhao, Y.; Hu, M.; Zhang, P.; Kong, N.; Liu, R.; Liu, C.; Choi, S. K. Lanthanide-doped core-shell nanoparticles as a multi-modality platform for imaging and photodynamic therapy. *Chem. Commun.* **2018**, *54*, 9525–9528.
- (47) Sun, J.; Zhang, P.; Fan, Y.; Zhao, J.; Niu, S.; Song, L.; Ma, L.; Ren, L.; Ming, W. Near-infrared triggered antibacterial nanocomposite membrane containing upconversion nanoparticles. *Mater. Sci. Eng., C* **2019**, *103*, 109797.
- (48) Zhang, Y.; Huang, P.; Wang, D.; Chen, J.; Liu, W.; Hu, P.; Huang, M.; Chen, X.; Chen, Z. Near-infrared-triggered antibacterial and antifungal photodynamic therapy based on lanthanide-doped upconversion nanoparticles. *Nanoscale* **2018**, *10*, 15485–15495.
- (49) Liu, W.; Zhang, Y.; You, W.; Su, J.; Yu, S.; Dai, T.; Huang, Y.; Chen, X.; Song, X.; Chen, Z. Near-infrared-excited upconversion photodynamic therapy of extensively drug-resistant *Acinetobacter baumannii* based on lanthanide nanoparticles. *Nanoscale* **2020**, *12*, 13948–13957.
- (50) Chen, X.; Peng, D.; Ju, Q.; Wang, F. Photon upconversion in core-shell nanoparticles. *Chem. Soc. Rev.* **2015**, *44*, 1318–1330.
- (51) Li, S.; Cui, S.; Yin, D.; Zhu, Q.; Ma, Y.; Qian, Z.; Gu, Y. Dual antibacterial activities of a chitosan-modified upconversion photodynamic therapy system against drug-resistant bacteria in deep tissue. *Nanoscale* **2017**, *9*, 3912–3924.
- (52) Xu, J.; Liu, N.; Wu, D.; Gao, Z.; Song, Y. Y.; Schmuki, P. Upconversion Nanoparticle-Assisted Payload Delivery from TiO₂ under Near-Infrared Light Irradiation for Bacterial Inactivation. *ACS Nano* **2020**, *14*, 337–346.
- (53) Ge, J.; Lan, M.; Zhou, B.; Liu, W.; Guo, L.; Wang, H.; Jia, Q.; Niu, G.; Huang, X.; Zhou, H.; Meng, X.; Wang, P.; Lee, C.-S.; Zhang, W.; Han, X. A graphene quantum dot photodynamic therapy agent with high singlet oxygen generation. *Nat. Commun.* **2014**, *5*, 4596.
- (54) Lee, E.; Li, X.; Oh, J.; Kwon, N.; Kim, G.; Kim, D.; Yoon, J. A boronic acid-functionalized phthalocyanine with an aggregation-enhanced photodynamic effect for combating antibiotic-resistant bacteria. *Chem. Sci.* **2020**, *11*, 5735–5739.
- (55) Sun, H.; Gao, N.; Dong, K.; Ren, J.; Qu, X. Graphene Quantum Dots-Band-Aids Used for Wound Disinfection. *ACS Nano* **2014**, *8*, 6202–6210.
- (56) Kuo, W. S.; Chang, C. Y.; Chen, H. H.; Hsu, C. L.; Wang, J. Y.; Kao, H. F.; Chou, L. C.; Chen, Y. C.; Chen, S. J.; Chang, W. T.; Tseng, S. W.; Wu, P. C.; Pu, Y. C. Two-Photon Photoexcited Photodynamic Therapy and Contrast Agent with Antimicrobial Graphene Quantum Dots. *ACS Appl. Mater. Interfaces* **2016**, *8*, 30467–30474.
- (57) Levy, M.; Bertram, J. R.; Eller, K. A.; Chatterjee, A.; Nagpal, P. Near-Infrared-Light-Triggered Antimicrobial Indium Phosphide Quantum Dots. *Angew. Chem., Int. Ed.* **2019**, *58*, 11414–11418.
- (58) Liu, J.; Liu, K.; Feng, L.; Liu, Z.; Xu, L. Comparison of nanomedicine-based chemotherapy, photodynamic therapy and photothermal therapy using reduced graphene oxide for the model system. *Biomater. Sci.* **2017**, *5*, 331–340.

- (59) Chen, Y.-W.; Su, Y.-L.; Hu, S.-H.; Chen, S.-Y. Functionalized graphene nanocomposites for enhancing photothermal therapy in tumor treatment. *Adv. Drug Delivery Rev.* **2016**, *105*, 190–204.
- (60) Zhang, Z.; Wang, Z.; Wang, F.; Ren, J.; Qu, X. Programmable Downregulation of Enzyme Activity Using a Fever and NIR-Responsive Molecularly Imprinted Nanocomposite. *Small* **2015**, *11*, 6172–6178.
- (61) Cui, T.; Wu, S.; Sun, Y.; Ren, J.; Qu, X. Self-Propelled Active Photothermal Nanoswimmer for Deep-Layered Elimination of Biofilm In Vivo. *Nano Lett.* **2020**, *20*, 7350–7358.
- (62) Chen, J.; Ning, C.; Zhou, C.; Yu, P.; Zhu, Y.; Tan, G.; Mao, C. Nanomaterials as photothermal therapeutic agents. *Prog. Mater. Sci.* **2019**, *99*, 1–26.
- (63) Pricker, S. P. Medical uses of gold compounds: Past, present and future. *Gold Bulletin* **1996**, *29*, 53–60.
- (64) Zhang, Z.; Zhao, A.; Wang, F.; Ren, J.; Qu, X. Design of a plasmonic micromotor for enhanced photo-remediation of polluted anaerobic stagnant waters. *Chem. Commun.* **2016**, *52*, 5550–5553.
- (65) Gwo, S.; Chen, H.-Y.; Lin, M.-H.; Sun, L.; Li, X. Nano-manipulation and controlled self-assembly of metal nanoparticles and nanocrystals for plasmonics. *Chem. Soc. Rev.* **2016**, *45*, 5672–5716.
- (66) Dreaden, E. C.; Alkilany, A. M.; Huang, X.; Murphy, C. J.; El-Sayed, M. A. The golden age: gold nanoparticles for biomedicine. *Chem. Soc. Rev.* **2012**, *41*, 2740–2779.
- (67) Zhao, Y.; Guo, Q.; Dai, X.; Wei, X.; Yu, Y.; Chen, X.; Li, C.; Cao, Z.; Zhang, X. A Biomimetic Non-Antibiotic Approach to Eradicate Drug-Resistant Infections. *Adv. Mater.* **2019**, *31*, 1806024.
- (68) Zhang, J.; Feng, Y.; Mi, J.; Shen, Y.; Tu, Z.; Liu, L. Photothermal lysis of pathogenic bacteria by platinum nanodots decorated gold nanorods under near infrared irradiation. *J. Hazard. Mater.* **2018**, *342*, 121–130.
- (69) Xie, Y.; Zheng, W.; Jiang, X. Near-Infrared Light-Activated Phototherapy by Gold Nanoclusters for Dispersing Biofilms. *ACS Appl. Mater. Interfaces* **2020**, *12*, 9041–9049.
- (70) Manivasagan, P.; Khan, F.; Hoang, G.; Mondal, S.; Kim, H.; Hoang Minh Doan, V.; Kim, Y. M.; Oh, J. Thiol chitosan-wrapped gold nanoshells for near-infrared laser-induced photothermal destruction of antibiotic-resistant bacteria. *Carbohydr. Polym.* **2019**, *225*, 115228.
- (71) Mahmoud, N. N.; Alkilany, A. M.; Khalil, E. A.; Al-Bakri, A. G. Nano-Photothermal Ablation Effect of Hydrophilic and Hydrophobic Functionalized Gold Nanorods on Staphylococcus aureus and Propionibacterium acnes. *Sci. Rep.* **2018**, *8*, 6881.
- (72) Aksoy, I.; Kucukkececi, H.; Sevgi, F.; Metin, O.; Hatay Patir, I. Photothermal Antibacterial and Antibiofilm Activity of Black Phosphorus/Gold Nanocomposites against Pathogenic Bacteria. *ACS Appl. Mater. Interfaces* **2020**, *12*, 26822–26831.
- (73) Mocan, L.; Matea, C.; Tabaran, F. A.; Mosteanu, O.; Pop, T.; Puia, C.; Agoston-Coldea, L.; Gonciar, D.; Kalman, E.; Zaharie, G.; Iancu, C.; Mocan, T. Selective in vitro photothermal nano-therapy of MRSA infections mediated by IgG conjugated gold nanoparticles. *Sci. Rep.* **2016**, *6*, 39466.
- (74) Teng, C. P.; Zhou, T.; Ye, E.; Liu, S.; Koh, L. D.; Low, M.; Loh, X. J.; Win, K. Y.; Zhang, L.; Han, M. Y. Effective Targeted Photothermal Ablation of Multidrug Resistant Bacteria and Their Biofilms with NIR-Absorbing Gold Nanocrosses. *Adv. Healthcare Mater.* **2016**, *5*, 2122–30.
- (75) Alhmoud, H.; Cifuentes-Rius, A.; Delalat, B.; Lancaster, D. G.; Voelcker, N. H. Gold-Decorated Porous Silicon Nanopillars for Targeted Hyperthermal Treatment of Bacterial Infections. *ACS Appl. Mater. Interfaces* **2017**, *9*, 33707–33716.
- (76) Ocsoy, I.; Yusufbeyoglu, S.; Yilmaz, V.; McLamore, E. S.; Ildiz, N.; Ulgen, A. DNA aptamer functionalized gold nanostructures for molecular recognition and photothermal inactivation of methicillin-resistant Staphylococcus aureus. *Colloids Surf., B* **2017**, *159*, 16–22.
- (77) Peng, Y.; Liu, Y.; Lu, X.; Wang, S.; Chen, M.; Huang, W.; Wu, Z.; Lu, G.; Nie, L. Ag-Hybridized plasmonic Au-triangular nanoplates: highly sensitive photoacoustic/Raman evaluation and improved antibacterial/photothermal combination therapy. *J. Mater. Chem. B* **2018**, *6*, 2813–2820.
- (78) Ma, K.; Li, Y.; Wang, Z.; Chen, Y.; Zhang, X.; Chen, C.; Yu, H.; Huang, J.; Yang, Z.; Wang, X.; Wang, Z. Core-Shell Gold Nanorod@ Layered Double Hydroxide Nanomaterial with Highly Efficient Photothermal Conversion and Its Application in Antibacterial and Tumor Therapy. *ACS Appl. Mater. Interfaces* **2019**, *11*, 29630–29640.
- (79) Mahmoud, N. N.; Alhusban, A. A.; Ali, J. I.; Al-Bakri, A. G.; Hamed, R.; Khalil, E. A. Preferential Accumulation of Phospholipid-PEG and Cholesterol-PEG Decorated Gold Nanorods into Human Skin Layers and Their Photothermal-Based Antibacterial Activity. *Sci. Rep.* **2019**, *9*, 5796.
- (80) Liao, Z.; Zhang, W.; Qiao, Z.; Luo, J.; Ai Niwaer, A. E.; Meng, X.; Wang, H.; Li, X.; Zuo, F.; Zhao, Z. Dopamine-assisted one-pot synthesis of gold nanoworms and their application as photothermal agents. *J. Colloid Interface Sci.* **2020**, *562*, 81–90.
- (81) Du, X.; Wang, W.; Wu, C.; Jia, B.; Li, W.; Qiu, L.; Jiang, P.; Wang, J.; Li, Y. Q. Enzyme-responsive turn-on nanoprobe for in situ fluorescence imaging and localized photothermal treatment of multidrug-resistant bacterial infections. *J. Mater. Chem. B* **2020**, *8*, 7403–7412.
- (82) Zhao, Q.; Wang, J.; Yin, C.; Zhang, P.; Zhang, J.; Shi, M.; Shen, K.; Xiao, Y.; Zhao, Y.; Yang, X.; Zhang, Y. Near-Infrared Light-Sensitive Nano Neuro-Immune Blocker Capsule Relieves Pain and Enhances the Innate Immune Response for Necrotizing Infection. *Nano Lett.* **2019**, *19*, 5904–5914.
- (83) Zou, X.; Zhang, L.; Wang, Z.; Luo, Y. Mechanisms of the Antimicrobial Activities of Graphene Materials. *J. Am. Chem. Soc.* **2016**, *138*, 2064–2077.
- (84) Lin, D.; Qin, T.; Wang, Y.; Sun, X.; Chen, L. Graphene oxide wrapped SERS tags: multifunctional platforms toward optical labeling, photothermal ablation of bacteria, and the monitoring of killing effect. *ACS Appl. Mater. Interfaces* **2014**, *6*, 1320–9.
- (85) Jia, X.; Ahmad, I.; Yang, R.; Wang, C. Versatile graphene-based photothermal nanocomposites for effectively capturing and killing bacteria, and for destroying bacterial biofilms. *J. Mater. Chem. B* **2017**, *5*, 2459–2467.
- (86) Li, M.; Yang, X.; Ren, J.; Qu, K.; Qu, X. Using Graphene Oxide High Near-Infrared Absorbance for Photothermal Treatment of Alzheimer's Disease. *Adv. Mater.* **2012**, *24*, 1722–1728.
- (87) Wang, Y. W.; Fu, Y. Y.; Wu, L. J.; Li, J.; Yang, H. H.; Chen, G. N. Targeted photothermal ablation of pathogenic bacterium, Staphylococcus aureus, with nanoscale reduced graphene oxide. *J. Mater. Chem. B* **2013**, *1*, 2496–2501.
- (88) Qian, W.; Yan, C.; He, D.; Yu, X.; Yuan, L.; Liu, M.; Luo, G.; Deng, J. pH-triggered charge-reversible of glycol chitosan conjugated carboxyl graphene for enhancing photothermal ablation of focal infection. *Acta Biomater.* **2018**, *69*, 256–264.
- (89) Liu, Z.; Liu, J.; Wang, R.; Du, Y.; Ren, J.; Qu, X. An efficient nano-based theranostic system for multi-modal imaging-guided photothermal sterilization in gastrointestinal tract. *Biomaterials* **2015**, *56*, 206–18.
- (90) Shan, J.; Yang, K.; Xiu, W.; Qiu, Q.; Dai, S.; Yuwen, L.; Weng, L.; Teng, Z.; Wang, L. Cu₂MoS₄ Nanozyme with NIR-II Light Enhanced Catalytic Activity for Efficient Eradication of Multidrug-Resistant Bacteria. *Small* **2020**, *16*, 2001099.
- (91) Zhu, C.; Shen, H.; Liu, H.; Lv, X.; Li, Z.; Yuan, Q. Solution-Processable Two-Dimensional In₂Se₃ Nanosheets as Efficient Photothermal Agents for Elimination of Bacteria. *Chem. - Eur. J.* **2018**, *24*, 19060.
- (92) Zhao, Y.; Wang, X.; Gao, F.; Wang, C.; Yang, Z.; Wu, H.; Li, C.; Cheng, L.; Peng, R. Facile Preparation of Cu₂Se Nanosheets as Dual-Functional Antibacterial Agents. *ACS Appl. Bio Mater.* **2020**, *3*, 1418–1425.
- (93) Zhang, W.; Shi, S.; Wang, Y.; Yu, S.; Zhu, W.; Zhang, X.; Zhang, D.; Yang, B.; Wang, X.; Wang, J. Versatile molybdenum disulfide based antibacterial composites for in vitro enhanced sterilization and in vivo focal infection therapy. *Nanoscale* **2016**, *8*, 11642–8.
- (94) Jeong, C. J.; Sharker, S. M.; In, I.; Park, S. Y. Iron Oxide@ PEDOT-Based Recyclable Photothermal Nanoparticles with Poly-

(vinylpyrrolidone) Sulfobetaines for Rapid and Effective Antibacterial Activity. *ACS Appl. Mater. Interfaces* **2015**, *7*, 9469–78.

(95) Jin, Y.; Deng, J.; Yu, J.; Yang, C.; Tong, M.; Hou, Y. Fe₅C₂ nanoparticles: a reusable bactericidal material with photothermal effects under near-infrared irradiation. *J. Mater. Chem. B* **2015**, *3*, 3993–4000.

(96) Huang, J.; Zhou, J.; Zhuang, J.; Gao, H.; Huang, D.; Wang, L.; Wu, W.; Li, Q.; Yang, D. P.; Han, M. Y. Strong Near-Infrared Absorbing and Biocompatible CuS Nanoparticles for Rapid and Efficient Photothermal Ablation of Gram-Positive and -Negative Bacteria. *ACS Appl. Mater. Interfaces* **2017**, *9*, 36606–36614.

(97) Ju, E.; Li, Z.; Li, M.; Dong, K.; Ren, J.; Qu, X. Functional polypyrrole-silica composites as photothermal agents for targeted killing of bacteria. *Chem. Commun.* **2013**, *49*, 9048–50.

(98) Feng, L.; Zhu, C.; Yuan, H.; Liu, L.; Lv, F.; Wang, S. Conjugated polymer nanoparticles: preparation, properties, functionalization and biological applications. *Chem. Soc. Rev.* **2013**, *42*, 6620–6633.

(99) Wang, Y.; Li, S.; Liu, L.; Feng, L. Photothermal-Responsive Conjugated Polymer Nanoparticles for the Rapid and Effective Killing of Bacteria. *ACS Appl. Bio Mater.* **2018**, *1*, 27–32.

(100) Ju, E.; Dong, K.; Liu, Z.; Pu, F.; Ren, J.; Qu, X. Tumor Microenvironment Activated Photothermal Strategy for Precisely Controlled Ablation of Solid Tumors upon NIR Irradiation. *Adv. Funct. Mater.* **2015**, *25*, 1574–1580.

(101) Abel, S. B.; Yslas, E. I.; Rivarola, C. R.; Barbero, C. A. Synthesis of polyaniline (PANI) and functionalized polyaniline (F-PANI) nanoparticles with controlled size by solvent displacement method. Application in fluorescence detection and bacteria killing by photothermal effect. *Nanotechnology* **2018**, *29*, 125604.

(102) Korupalli, C.; Huang, C. C.; Lin, W. C.; Pan, W. Y.; Lin, P. Y.; Wan, W. L.; Li, M. J.; Chang, Y.; Sung, H. W. Acidity-triggered charge-convertible nanoparticles that can cause bacterium-specific aggregation in situ to enhance photothermal ablation of focal infection. *Biomaterials* **2017**, *116*, 1–9.

(103) Yang, Q.; Ma, Z.; Wang, H.; Zhou, B.; Zhu, S.; Zhong, Y.; Wang, J.; Wan, H.; Antaris, A.; Ma, R.; Zhang, X.; Yang, J.; Zhang, X.; Sun, H.; Liu, W.; Liang, Y.; Dai, H. Rational Design of Molecular Fluorophores for Biological Imaging in the NIR-II Window. *Adv. Mater.* **2017**, *29*, 1605497.

(104) Cekli, S.; Winkel, R. W.; Alarousu, E.; Mohammed, O. F.; Schanze, K. S. Triplet excited state properties in variable gap π -conjugated donor–acceptor–donor chromophores. *Chem. Sci.* **2016**, *7*, 3621–3631.

(105) Wang, B.; Feng, G.; Seifrid, M.; Wang, M.; Liu, B.; Bazan, G. C. Antibacterial Narrow-Band-Gap Conjugated Oligoelectrolytes with High Photothermal Conversion Efficiency. *Angew. Chem., Int. Ed.* **2017**, *56*, 16063–16066.

(106) Jiao, Y.; Liu, K.; Wang, G.; Wang, Y.; Zhang, X. Supramolecular free radicals: near-infrared organic materials with enhanced photothermal conversion. *Chem. Sci.* **2015**, *6*, 3975–3980.

(107) Yang, Y.; He, P.; Wang, Y.; Bai, H.; Wang, S.; Xu, J. F.; Zhang, X. Supramolecular Radical Anions Triggered by Bacteria In Situ for Selective Photothermal Therapy. *Angew. Chem., Int. Ed.* **2017**, *56*, 16239–16242.

(108) Yao, J.; Yang, M.; Duan, Y. Chemistry, Biology, and Medicine of Fluorescent Nanomaterials and Related Systems: New Insights into Biosensing, Bioimaging, Genomics, Diagnostics, and Therapy. *Chem. Rev.* **2014**, *114*, 6130–6178.

(109) Turcheniuk, K.; Hage, C. H.; Spadavecchia, J.; Serrano, A. Y.; Larroulet, I.; Pesquera, A.; Zurutuza, A.; Pisfil, M. G.; Heliot, L.; Boukaert, J.; Boukherroub, R.; Szunerits, S. Plasmonic photothermal destruction of uropathogenic *E. coli* with reduced graphene oxide and core/shell nanocomposites of gold nanorods/reduced graphene oxide. *J. Mater. Chem. B* **2015**, *3*, 375–386.

(110) Liu, D.; Ma, L.; Liu, L.; Wang, L.; Liu, Y.; Jia, Q.; Guo, Q.; Zhang, G.; Zhou, J. Polydopamine-Encapsulated Fe₃O₄ with an Adsorbed HSP70 Inhibitor for Improved Photothermal Inactivation of Bacteria. *ACS Appl. Mater. Interfaces* **2016**, *8*, 24455–62.

(111) Yang, Y.; Ma, L.; Cheng, C.; Deng, Y.; Huang, J.; Fan, X.; Nie, C.; Zhao, W.; Zhao, C. Nonchemotherapeutic and Robust Dual-Responsive Nanoagents with On-Demand Bacterial Trapping, Ablation, and Release for Efficient Wound Disinfection. *Adv. Funct. Mater.* **2018**, *28*, 1705708.

(112) Chen, G.; Qiu, H.; Prasad, P. N.; Chen, X. Upconversion Nanoparticles: Design, Nanochemistry, and Applications in Theranostics. *Chem. Rev.* **2014**, *114*, 5161–5214.

(113) Wang, Z.; Hu, M.; Ai, X.; Zhang, Z.; Xing, B. Near-Infrared Manipulation of Membrane Ion Channels via Upconversion Optogenetics. *Adv. Biosyst.* **2019**, *3*, 1800233.

(114) Lyu, L.; Cheong, H.; Ai, X.; Zhang, W.; Li, J.; Yang, H.; Lin, J.; Xing, B. Near-infrared light-mediated rare-earth nanocrystals: recent advances in improving photon conversion and alleviating the thermal effect. *NPG Asia Mater.* **2018**, *10*, 685–702.

(115) Ai, X.; Lyu, L.; Zhang, Y.; Tang, Y.; Mu, J.; Liu, F.; Zhou, Y.; Zuo, Z.; Liu, G.; Xing, B. Remote Regulation of Membrane Channel Activity by Site-Specific Localization of Lanthanide-Doped Upconversion Nanocrystals. *Angew. Chem., Int. Ed.* **2017**, *56*, 3031–3035.

(116) Ai, X.; Ho, C. J. H.; Aw, J.; Attia, A. B. E.; Mu, J.; Wang, Y.; Wang, X.; Wang, Y.; Liu, X.; Chen, H.; Gao, M.; Chen, X.; Yeow, E. K. L.; Liu, G.; Olivo, M.; Xing, B. In vivo covalent cross-linking of photon-converted rare-earth nanostructures for tumour localization and theranostics. *Nat. Commun.* **2016**, *7*, 10432.

(117) Ai, X.; Wang, Z.; Cheong, H.; Wang, Y.; Zhang, R.; Lin, J.; Zheng, Y.; Gao, M.; Xing, B. Multispectral optoacoustic imaging of dynamic redox correlation and pathophysiological progression utilizing upconversion nanoprobes. *Nat. Commun.* **2019**, *10*, 1087.

(118) Suo, H.; Zhao, X.; Zhang, Z.; Guo, C. 808 nm Light-Triggered Thermometer-Heater Upconverting Platform Based on Nd(3+)-Sensitized Yolk-Shell GdOF@SiO₂. *ACS Appl. Mater. Interfaces* **2017**, *9*, 43438–43448.

(119) Suo, H.; Zhao, X.; Zhang, Z.; Wu, Y.; Guo, C. Upconverting LuVO₄:Nd(3+)/Yb(3+)/Er(3+)@SiO₂@Cu₂S Hollow Nanoplat-forms for Self-monitored Photothermal Ablation. *ACS Appl. Mater. Interfaces* **2018**, *10*, 39912–39920.

(120) Zhang, Z.; Suo, H.; Zhao, X.; Sun, D.; Fan, L.; Guo, C. NIR-to-NIR Deep Penetrating Nanoplat-forms Y₂O₃:Nd(3+)/Yb(3+)@SiO₂@Cu₂S toward Highly Efficient Photothermal Ablation. *ACS Appl. Mater. Interfaces* **2018**, *10*, 14570–14576.

(121) Zhao, Z.; Yan, R.; Yi, X.; Li, J.; Rao, J.; Guo, Z.; Yang, Y.; Li, W.; Li, Y. Q.; Chen, C. Bacteria-Activated Theranostic Nanoprobes against Methicillin-Resistant *Staphylococcus aureus* Infection. *ACS Nano* **2017**, *11*, 4428–4438.

(122) Yang, X.; Li, Z.; Ju, E.; Ren, J.; Qu, X. Reduced graphene oxide functionalized with a luminescent rare-earth complex for the tracking and photothermal killing of drug-resistant bacteria. *Chem. - Eur. J.* **2014**, *20*, 394–8.

(123) Tao, B.; Lin, C.; Yuan, Z.; He, Y.; Chen, M.; Li, K.; Hu, J.; Yang, Y.; Xia, Z.; Cai, K. Near infrared light-triggered on-demand Cur release from Gel-PDA@Cur composite hydrogel for antibacterial wound healing. *Chem. Eng. J.* **2021**, *403*, 126182.

(124) Sasidharan, S.; Poojari, R.; Bahadur, D.; Srivastava, R. Embelin-Mediated Green Synthesis of Quasi-Spherical and Star-Shaped Plasmonic Nanostructures for Antibacterial Activity, Photothermal Therapy, and Computed Tomographic Imaging. *ACS Sustainable Chem. Eng.* **2018**, *6*, 10562–10577.

(125) Li, L.; Fu, L.; Ai, X.; Zhang, J.; Zhou, J. Design and Fabrication of Temperature-Sensitive Nanogels with Controlled Drug Release Properties for Enhanced Photothermal Sterilization. *Chem. - Eur. J.* **2017**, *23*, 18180–18186.

(126) Ji, H.; Dong, K.; Yan, Z.; Ding, C.; Chen, Z.; Ren, J.; Qu, X. Bacterial Hyaluronidase Self-Triggered Prodrug Release for Chemo-Photothermal Synergistic Treatment of Bacterial Infection. *Small* **2016**, *12*, 6200–6206.

(127) Huang, Y.; Gao, Q.; Li, X.; Gao, Y.; Han, H.; Jin, Q.; Yao, K.; Ji, J. Ofloxacin loaded MoS₂ nanoflakes for synergistic mild-temperature photothermal/antibiotic therapy with reduced drug resistance of bacteria. *Nano Res.* **2020**, *13*, 2340–2350.

- (128) Guo, Z.; He, J. X.; Mahadevegowda, S. H.; Kho, S. H.; Chan-Park, M. B.; Liu, X. W. Multifunctional Glyco-Nanosheets to Eradicate Drug-Resistant Bacteria on Wounds. *Adv. Healthcare Mater.* **2020**, *9*, 2000265.
- (129) Guo, X.; Cao, B.; Wang, C.; Lu, S.; Hu, X. In vivo photothermal inhibition of methicillin-resistant *Staphylococcus aureus* infection by in situ templated formulation of pathogen-targeting phototheranostics. *Nanoscale* **2020**, *12*, 7651–7659.
- (130) Gao, G.; Jiang, Y. W.; Jia, H. R.; Wu, F. G. Near-infrared light-controllable on-demand antibiotics release using thermo-sensitive hydrogel-based drug reservoir for combating bacterial infection. *Biomaterials* **2019**, *188*, 83–95.
- (131) Moorcroft, S. C. T.; Roach, L.; Jayne, D. G.; Ong, Z. Y.; Evans, S. D. Nanoparticle-Loaded Hydrogel for the Light-Activated Release and Photothermal Enhancement of Antimicrobial Peptides. *ACS Appl. Mater. Interfaces* **2020**, *12*, 24544–24554.
- (132) Tan, L.; Zhou, Z.; Liu, X.; Li, J.; Zheng, Y.; Cui, Z.; Yang, X.; Liang, Y.; Li, Z.; Feng, X.; Zhu, S.; Yeung, K. W. K.; Yang, C.; Wang, X.; Wu, S. Overcoming Multidrug-Resistant MRSA Using Conventional Aminoglycoside Antibiotics. *Adv. Sci.* **2020**, *7*, 1902070.
- (133) Zhang, C.; Hu, D. F.; Xu, J. W.; Ma, M. Q.; Xing, H.; Yao, K.; Ji, J.; Xu, Z. K. Polyphenol-Assisted Exfoliation of Transition Metal Dichalcogenides into Nanosheets as Photothermal Nanocarriers for Enhanced Antibiofilm Activity. *ACS Nano* **2018**, *12*, 12347–12356.
- (134) Zhao, Y.; Dai, X.; Wei, X.; Yu, Y.; Chen, X.; Zhang, X.; Li, C. Near-Infrared Light-Activated Thermosensitive Liposomes as Efficient Agents for Photothermal and Antibiotic Synergistic Therapy of Bacterial Biofilm. *ACS Appl. Mater. Interfaces* **2018**, *10*, 14426–14437.
- (135) Zhang, L.; Wang, Y.; Wang, J.; Wang, Y.; Chen, A.; Wang, C.; Mo, W.; Li, Y.; Yuan, Q.; Zhang, Y. Photon-Responsive Antibacterial Nanoplatfor for Synergistic Photothermal-/Pharmaco-Therapy of Skin Infection. *ACS Appl. Mater. Interfaces* **2019**, *11*, 300–310.
- (136) Zhang, L.; Wang, Y.; Wang, C.; He, M.; Wan, J.; Wei, Y.; Zhang, J.; Yang, X.; Zhao, Y.; Zhang, Y. Light-Activable On-Demand Release of Nano-Antibiotic Platforms for Precise Synergy of Thermochemotherapy on Periodontitis. *ACS Appl. Mater. Interfaces* **2020**, *12*, 3354–3362.
- (137) Wang, W.-N.; Zhang, C.-Y.; Zhang, M.-F.; Pei, P.; Zhou, W.; Zha, Z.-B.; Shao, M.; Qian, H.-S. Precisely photothermal controlled releasing of antibacterial agent from Bi2S3 hollow microspheres triggered by NIR light for water sterilization. *Chem. Eng. J.* **2020**, *381*, 122630.
- (138) Wang, C.; Wang, Y.; Zhang, L.; Miron, R. J.; Liang, J.; Shi, M.; Mo, W.; Zheng, S.; Zhao, Y.; Zhang, Y. Pretreated Macrophage-Membrane-Coated Gold Nanocages for Precise Drug Delivery for Treatment of Bacterial Infections. *Adv. Mater.* **2018**, *30*, 1804023.
- (139) Qing, G.; Zhao, X.; Gong, N.; Chen, J.; Li, X.; Gan, Y.; Wang, Y.; Zhang, Z.; Zhang, Y.; Guo, W.; Luo, Y.; Liang, X. J. Thermo-responsive triple-function nanotransporter for efficient chemo-photothermal therapy of multidrug-resistant bacterial infection. *Nat. Commun.* **2019**, *10*, 4336.
- (140) Liu, Y.; Lin, A.; Liu, J.; Chen, X.; Zhu, X.; Gong, Y.; Yuan, G.; Chen, L.; Liu, J. Enzyme-Responsive Mesoporous Ruthenium for Combined Chemo-Photothermal Therapy of Drug-Resistant Bacteria. *ACS Appl. Mater. Interfaces* **2019**, *11*, 26590–26606.
- (141) He, D.; Yang, T.; Qian, W.; Qi, C.; Mao, L.; Yu, X.; Zhu, H.; Luo, G.; Deng, J. Combined photothermal and antibiotic therapy for bacterial infection via acidity-sensitive nanocarriers with enhanced antimicrobial performance. *Applied Materials Today* **2018**, *12*, 415–429.
- (142) Shi, M.; Zhang, P.; Zhao, Q.; Shen, K.; Qiu, Y.; Xiao, Y.; Yuan, Q.; Zhang, Y. Dual Functional Monocytes Modulate Bactericidal and Anti-Inflammation Process for Severe Osteomyelitis Treatment. *Small* **2020**, *16*, 1905185.
- (143) Cao, C.; Ge, W.; Yin, J.; Yang, D.; Wang, W.; Song, X.; Hu, Y.; Yin, J.; Dong, X. Mesoporous Silica Supported Silver-Bismuth Nanoparticles as Photothermal Agents for Skin Infection Synergistic Antibacterial Therapy. *Small* **2020**, *16*, 2000436.
- (144) Hu, B.; Wang, N.; Han, L.; Chen, M. L.; Wang, J. H. Core-shell nanoheater for photothermal treatment on bacteria. *Acta Biomater.* **2015**, *11*, 511–9.
- (145) Hu, B.; Wang, N.; Han, L.; Chen, M. L.; Wang, J. H. Magnetic nanohybrids loaded with bimetal core-shell-shell nanorods for bacteria capture, separation, and near-infrared photothermal treatment. *Chem. - Eur. J.* **2015**, *21*, 6582–9.
- (146) Hu, X.; Zhao, Y.; Hu, Z.; Saran, A.; Hou, S.; Wen, T.; Liu, W.; Ji, Y.; Jiang, X.; Wu, X. Gold nanorods core/AgPt alloy nanodots shell: A novel potent antibacterial nanostructure. *Nano Res.* **2013**, *6*, 822–835.
- (147) Mei, Z.; Gao, D.; Hu, D.; Zhou, H.; Ma, T.; Huang, L.; Liu, X.; Zheng, R.; Zheng, H.; Zhao, P.; Zhou, J.; Sheng, Z. Activatable NIR-II photoacoustic imaging and photochemical synergistic therapy of MRSA infections using miniature Au/Ag nanorods. *Biomaterials* **2020**, *251*, 120092.
- (148) Mo, S.; Chen, X.; Chen, M.; He, C.; Lu, Y.; Zheng, N. Two-dimensional antibacterial Pd@Ag nanosheets with a synergetic effect of plasmonic heating and Ag(+) release. *J. Mater. Chem. B* **2015**, *3*, 6255–6260.
- (149) Qiao, Y.; Ma, F.; Liu, C.; Zhou, B.; Wei, Q.; Li, W.; Zhong, D.; Li, Y.; Zhou, M. Near-Infrared Laser-Excited Nanoparticles To Eradicate Multidrug-Resistant Bacteria and Promote Wound Healing. *ACS Appl. Mater. Interfaces* **2018**, *10*, 193–206.
- (150) Xu, Q.; Chang, M.; Zhang, Y.; Wang, E.; Xing, M.; Gao, L.; Huan, Z.; Guo, F.; Chang, J. PDA/Cu Bioactive Hydrogel with "Hot Ions Effect" for Inhibition of Drug-Resistant Bacteria and Enhancement of Infectious Skin Wound Healing. *ACS Appl. Mater. Interfaces* **2020**, *12*, 31255–31269.
- (151) Fuhrmann, G.-F.; Rothstein, A. The mechanism of the partial inhibition of fermentation in yeast by nickel ions. *Biochim. Biophys. Acta, Biomembr.* **1968**, *163*, 331–338.
- (152) Feng, Q. L.; Wu, J.; Chen, G. Q.; Cui, F. Z.; Kim, T. N.; Kim, J. O. A mechanistic study of the antibacterial effect of silver ions on *Escherichia coli* and *Staphylococcus aureus*. *J. Biomed. Mater. Res.* **2000**, *52*, 662–668.
- (153) Ran, X.; Du, Y.; Wang, Z.; Wang, H.; Pu, F.; Ren, J.; Qu, X. Hyaluronic Acid-Templated Ag Nanoparticles/Graphene Oxide Composites for Synergistic Therapy of Bacteria Infection. *ACS Appl. Mater. Interfaces* **2017**, *9*, 19717–19724.
- (154) Yuwen, L.; Sun, Y.; Tan, G.; Xiu, W.; Zhang, Y.; Weng, L.; Teng, Z.; Wang, L. MoS₂@polydopamine-Ag nanosheets with enhanced antibacterial activity for effective treatment of *Staphylococcus aureus* biofilms and wound infection. *Nanoscale* **2018**, *10*, 16711–16720.
- (155) Fan, X.; Yang, F.; Nie, C.; Yang, Y.; Ji, H.; He, C.; Cheng, C.; Zhao, C. Mussel-Inspired Synthesis of NIR-Responsive and Biocompatible Ag-Graphene 2D Nanoagents for Versatile Bacterial Disinfections. *ACS Appl. Mater. Interfaces* **2018**, *10*, 296–307.
- (156) Gong, P.; Wang, F.; Guo, F.; Liu, J.; Wang, B.; Ge, X.; Li, S.; You, J.; Liu, Z. Fluorescence turn-off Ag/fluorinated graphene composites with high NIR absorption for effective killing of cancer cells and bacteria. *J. Mater. Chem. B* **2018**, *6*, 7926–7935.
- (157) Wu, S.; Li, A.; Zhao, X.; Zhang, C.; Yu, B.; Zhao, N.; Xu, F. J. Silica-Coated Gold-Silver Nanocages as Photothermal Antibacterial Agents for Combined Anti-Infective Therapy. *ACS Appl. Mater. Interfaces* **2019**, *11*, 17177–17183.
- (158) Qiao, Y.; He, J.; Chen, W.; Yu, Y.; Li, W.; Du, Z.; Xie, T.; Ye, Y.; Hua, S. Y.; Zhong, D.; Yao, K.; Zhou, M. Light-Activatable Synergistic Therapy of Drug-Resistant Bacteria-Infected Cutaneous Chronic Wounds and Nonhealing Keratitis by Cupriferous Hollow Nanoshells. *ACS Nano* **2020**, *14*, 3299–3315.
- (159) Qiao, Y.; Ping, Y.; Zhang, H.; Zhou, B.; Liu, F.; Yu, Y.; Xie, T.; Li, W.; Zhong, D.; Zhang, Y.; Yao, K.; Santos, H. A.; Zhou, M. Laser-Activatable CuS Nanodots to Treat Multidrug-Resistant Bacteria and Release Copper Ion to Accelerate Healing of Infected Chronic Nonhealing Wounds. *ACS Appl. Mater. Interfaces* **2019**, *11*, 3809–3822.
- (160) Fan, X.; Yang, F.; Huang, J.; Yang, Y.; Nie, C.; Zhao, W.; Ma, L.; Cheng, C.; Zhao, C.; Haag, R. Metal-Organic-Framework-Derived 2D Carbon Nanosheets for Localized Multiple Bacterial Eradication and Augmented Anti-infective Therapy. *Nano Lett.* **2019**, *19*, 5885–5896.

- (161) Yang, Y.; Deng, Y.; Huang, J.; Fan, X.; Cheng, C.; Nie, C.; Ma, L.; Zhao, W.; Zhao, C. Size-Transformable Metal–Organic Framework–Derived Nanocarbons for Localized Chemo-Photothermal Bacterial Ablation and Wound Disinfection. *Adv. Funct. Mater.* **2019**, *29*, 1900143.
- (162) Li, J.; Liu, X.; Tan, L.; Cui, Z.; Yang, X.; Liang, Y.; Li, Z.; Zhu, S.; Zheng, Y.; Yeung, K. W. K.; Wang, X.; Wu, S. Zinc-doped Prussian blue enhances photothermal clearance of *Staphylococcus aureus* and promotes tissue repair in infected wounds. *Nat. Commun.* **2019**, *10*, 4490.
- (163) Huang, Y.; Ren, J.; Qu, X. Nanozymes: Classification, Catalytic Mechanisms, Activity Regulation, and Applications. *Chem. Rev.* **2019**, *119*, 4357–4412.
- (164) Yin, W.; Yu, J.; Lv, F.; Yan, L.; Zheng, L. R.; Gu, Z.; Zhao, Y. Functionalized Nano-MoS₂ with Peroxidase Catalytic and Near-Infrared Photothermal Activities for Safe and Synergetic Wound Antibacterial Applications. *ACS Nano* **2016**, *10*, 11000–11011.
- (165) Huo, M.; Wang, L.; Zhang, H.; Zhang, L.; Chen, Y.; Shi, J. Construction of Single-Iron-Atom Nanocatalysts for Highly Efficient Catalytic Antibiotics. *Small* **2019**, *15*, 1901834.
- (166) Liu, Y.; Guo, Z.; Li, F.; Xiao, Y.; Zhang, Y.; Bu, T.; Jia, P.; Zhe, T.; Wang, L. Multifunctional Magnetic Copper Ferrite Nanoparticles as Fenton-like Reaction and Near-Infrared Photothermal Agents for Synergetic Antibacterial Therapy. *ACS Appl. Mater. Interfaces* **2019**, *11*, 31649–31660.
- (167) Li, D.; Fang, Y.; Zhang, X. Bacterial Detection and Elimination Using a Dual-Functional Porphyrin-Based Porous Organic Polymer with Peroxidase-Like and High Near-Infrared-Light-Enhanced Antibacterial Activity. *ACS Appl. Mater. Interfaces* **2020**, *12*, 8989–8999.
- (168) Cao, F.; Zhang, L.; Wang, H.; You, Y.; Wang, Y.; Gao, N.; Ren, J.; Qu, X. Defect-Rich Adhesive Nanozymes as Efficient Antibiotics for Enhanced Bacterial Inhibition. *Angew. Chem., Int. Ed.* **2019**, *58*, 16236–16242.
- (169) Zhao, B.; Wang, H.; Dong, W.; Cheng, S.; Li, H.; Tan, J.; Zhou, J.; He, W.; Li, L.; Zhang, J.; Luo, G.; Qian, W. A multifunctional platform with single-NIR-laser-triggered photothermal and NO release for synergistic therapy against multidrug-resistant Gram-negative bacteria and their biofilms. *J. Nanobiotechnol.* **2020**, *18*, 59.
- (170) Ma, W.; Chen, X.; Fu, L.; Zhu, J.; Fan, M.; Chen, J.; Yang, C.; Yang, G.; Wu, L.; Mao, G.; Yang, X.; Mou, X.; Gu, Z.; Cai, X. Ultra-efficient Antibacterial System Based on Photodynamic Therapy and CO Gas Therapy for Synergistic Antibacterial and Ablation Biofilms. *ACS Appl. Mater. Interfaces* **2020**, *12*, 22479–22491.
- (171) Fan, W.; Lu, N.; Huang, P.; Liu, Y.; Yang, Z.; Wang, S.; Yu, G.; Liu, Y.; Hu, J.; He, Q.; Qu, J.; Wang, T.; Chen, X. Glucose-Responsive Sequential Generation of Hydrogen Peroxide and Nitric Oxide for Synergistic Cancer Starving-Like/Gas Therapy. *Angew. Chem., Int. Ed.* **2017**, *56*, 1229–1233.
- (172) Yu, S.; Li, G.; Liu, R.; Ma, D.; Xue, W. Dendritic Fe₃O₄@Poly(dopamine)@PAMAM Nanocomposite as Controllable NO-Releasing Material: A Synergistic Photothermal and NO Antibacterial Study. *Adv. Funct. Mater.* **2018**, *28*, 1707440.
- (173) Liu, Y. T.; Shi, S. W.; Wang, Y.; Zhang, Q. L.; Gao, S. H.; Yang, S. P.; Liu, J. G. A Ruthenium Nitrosyl-Functionalized Magnetic Nanoparticle with Near-Infrared Light-Controlled Nitric Oxide Delivery and Photothermal Effect for Enhanced Antitumor and Antibacterial Therapy. *ACS Appl. Mater. Interfaces* **2020**, *12*, 312–321.
- (174) Gao, Q.; Zhang, X.; Yin, W.; Ma, D.; Xie, C.; Zheng, L.; Dong, X.; Mei, L.; Yu, J.; Wang, C.; Gu, Z.; Zhao, Y. Functionalized MoS₂ Nanovehicle with Near-Infrared Laser-Mediated Nitric Oxide Release and Photothermal Activities for Advanced Bacteria-Infected Wound Therapy. *Small* **2018**, *14*, 1802290.
- (175) Huang, S.; Liu, H.; Liao, K.; Hu, Q.; Guo, R.; Deng, K. Functionalized GO Nanovehicles with Nitric Oxide Release and Photothermal Activity-Based Hydrogels for Bacteria-Infected Wound Healing. *ACS Appl. Mater. Interfaces* **2020**, *12*, 28952–28964.
- (176) Yu, S.; Li, G.; Zhao, P.; Cheng, Q.; He, Q.; Ma, D.; Xue, W. NIR-Laser-Controlled Hydrogen-Releasing PdH Nanohydride for Synergistic Hydrogen-Photothermal Antibacterial and Wound-Healing Therapies. *Adv. Funct. Mater.* **2019**, *29*, 1905697.
- (177) Samal, S. K.; Dash, M.; Van Vlierberghe, S.; Kaplan, D. L.; Chiellini, E.; van Blitterswijk, C.; Moroni, L.; Dubruel, P. Cationic polymers and their therapeutic potential. *Chem. Soc. Rev.* **2012**, *41*, 7147–7194.
- (178) Hu, D.; Li, H.; Wang, B.; Ye, Z.; Lei, W.; Jia, F.; Jin, Q.; Ren, K. F.; Ji, J. Surface-Adaptive Gold Nanoparticles with Effective Adherence and Enhanced Photothermal Ablation of Methicillin-Resistant *Staphylococcus aureus* Biofilm. *ACS Nano* **2017**, *11*, 9330–9339.
- (179) Feng, G.; Mai, C. K.; Zhan, R.; Bazan, G. C.; Liu, B. Narrow band gap conjugated polyelectrolytes for photothermal killing of bacteria. *J. Mater. Chem. B* **2015**, *3*, 7340–7346.
- (180) Mazrad, Z. A. I.; Choi, C. A.; Kwon, Y. M.; In, I.; Lee, K. D.; Park, S. Y. Design of Surface-Coatable NIR-Responsive Fluorescent Nanoparticles with PEI Passivation for Bacterial Detection and Killing. *ACS Appl. Mater. Interfaces* **2017**, *9*, 33317–33326.
- (181) Yang, X.; Xia, P.; Zhang, Y.; Lian, S.; Li, H.; Zhu, G.; Wang, P. Photothermal Nano-antibiotic for Effective Treatment of Multidrug-Resistant Bacterial Infection. *ACS Appl. Bio Mater.* **2020**, *3*, 5395–5406.
- (182) Wang, H.; Zhao, B.; Dong, W.; Zhong, Y.; Zhang, X.; Gong, Y.; Zhan, R.; Xing, M.; Zhang, J.; Luo, G.; Qian, W. A dual-targeted platform based on graphene for synergistic chemo-photothermal therapy against multidrug-resistant Gram-negative bacteria and their biofilms. *Chem. Eng. J.* **2020**, *393*, 124595.
- (183) Yan, L. X.; Chen, L. J.; Zhao, X.; Yan, X. P. pH Switchable Nanoparticle for In Vivo Persistent Luminescence Imaging and Precise Photothermal Therapy of Bacterial Infection. *Adv. Funct. Mater.* **2020**, *30*, 1909042.
- (184) Li, J.; Liu, X.; Zhou, Z.; Tan, L.; Wang, X.; Zheng, Y.; Han, Y.; Chen, D. F.; Yeung, K. W. K.; Cui, Z.; Yang, X.; Liang, Y.; Li, Z.; Zhu, S.; Wu, S. Lysozyme-Assisted Photothermal Eradication of Methicillin-Resistant *Staphylococcus aureus* Infection and Accelerated Tissue Repair with Natural Melanosome Nanostructures. *ACS Nano* **2019**, *13*, 11153–11167.
- (185) Chen, Y.; Gao, Y.; Li, Y.; Wang, K.; Zhu, J. Synergistic chemo-photodynamic therapy mediated by light-activated ROS-degradable nanocarriers. *J. Mater. Chem. B* **2019**, *7*, 460–468.
- (186) Kalluru, P.; Vankayala, R.; Chiang, C.-S.; Hwang, K. C. Unprecedented “All-in-One” Lanthanide-Doped Mesoporous Silica Frameworks for Fluorescence/MR Imaging and Combination of NIR Light Triggered Chemo-Photodynamic Therapy of Tumors. *Adv. Funct. Mater.* **2016**, *26*, 7908–7920.
- (187) He, C.; Liu, D.; Lin, W. Self-Assembled Core–Shell Nanoparticles for Combined Chemotherapy and Photodynamic Therapy of Resistant Head and Neck Cancers. *ACS Nano* **2015**, *9*, 991–1003.
- (188) Zhao, J.; Xu, J.; Jian, X.; Xu, J.; Gao, Z.; Song, Y. Y. NIR Light-Driven Photocatalysis on Amphiphilic TiO₂ Nanotubes for Controllable Drug Release. *ACS Appl. Mater. Interfaces* **2020**, *12*, 23606–23616.
- (189) Wei, W.; Bing, W.; Ren, J.; Qu, X. Near infrared-caged d-amino acids multifunctional assembly for simultaneously eradicating biofilms and bacteria. *Chem. Commun.* **2015**, *51*, 12677–9.
- (190) Chen, H.; Yang, J.; Sun, L.; Zhang, H.; Guo, Y.; Qu, J.; Jiang, W.; Chen, W.; Ji, J.; Yang, Y.-W.; Wang, B. Synergistic Chemotherapy and Photodynamic Therapy of Endophthalmitis Mediated by Zeolitic Imidazolate Framework-Based Drug Delivery Systems. *Small* **2019**, *15*, 1903880.
- (191) Zhang, R.; Li, Y.; Zhou, M.; Wang, C.; Feng, P.; Miao, W.; Huang, H. Photodynamic Chitosan Nano-Assembly as a Potent Alternative Candidate for Combating Antibiotic-Resistant Bacteria. *ACS Appl. Mater. Interfaces* **2019**, *11*, 26711–26721.
- (192) Zhang, Y.; Sun, P.; Zhang, L.; Wang, Z.; Wang, F.; Dong, K.; Liu, Z.; Ren, J.; Qu, X. Silver-Infused Porphyrinic Metal–Organic Framework: Surface-Adaptive, On-Demand Nanoparticle for Synergistic Bacteria Killing and Wound Disinfection. *Adv. Funct. Mater.* **2019**, *29*, 1808594.

- (193) Xiao, X.; Hou, C.; Zhang, Z.; Ke, Z.; Lan, J.; Jiang, H.; Zeng, W. Iridium(III)-Catalyzed Regioselective Intermolecular Unactivated Secondary Csp³-H Bond Amidation. *Angew. Chem., Int. Ed.* **2016**, *55*, 11897–11901.
- (194) Sanz-Ortiz, M. N.; Sentosun, K.; Bals, S.; Liz-Marzán, L. M. Templated Growth of Surface Enhanced Raman Scattering-Active Branched Gold Nanoparticles within Radial Mesoporous Silica Shells. *ACS Nano* **2015**, *9*, 10489–10497.
- (195) Jiang, B.-P.; Zhang, L.; Guo, X.-L.; Shen, X.-C.; Wang, Y.; Zhu, Y.; Liang, H. Poly(N-phenylglycine)-Based Nanoparticles as Highly Effective and Targeted Near-Infrared Photothermal Therapy/Photodynamic Therapeutic Agents for Malignant Melanoma. *Small* **2017**, *13*, 1602496.
- (196) Cai, Y.; Liang, P.; Tang, Q.; Yang, X.; Si, W.; Huang, W.; Zhang, Q.; Dong, X. Diketopyrrolopyrrole-Triphenylamine Organic Nanoparticles as Multifunctional Reagents for Photoacoustic Imaging-Guided Photodynamic/Photothermal Synergistic Tumor Therapy. *ACS Nano* **2017**, *11*, 1054–1063.
- (197) Dai, X.; Zhao, Y.; Yu, Y.; Chen, X.; Wei, X.; Zhang, X.; Li, C. Single Continuous Near-Infrared Laser-Triggered Photodynamic and Photothermal Ablation of Antibiotic-Resistant Bacteria Using Effective Targeted Copper Sulfide Nanoclusters. *ACS Appl. Mater. Interfaces* **2017**, *9*, 30470–30479.
- (198) Dai, X.; Zhao, Y.; Yu, Y.; Chen, X.; Wei, X.; Zhang, X.; Li, C. All-in-one NIR-activated nanoplatfoms for enhanced bacterial biofilm eradication. *Nanoscale* **2018**, *10*, 18520–18530.
- (199) Fan, H.; Fan, Y.; Du, W.; Cai, R.; Gao, X.; Liu, X.; Wang, H.; Wang, L.; Wu, X. Enhanced type I photoreaction of indocyanine green via electrostatic-force-driven aggregation. *Nanoscale* **2020**, *12*, 9517–9523.
- (200) Huang, X.; Chen, G.; Pan, J.; Chen, X.; Huang, N.; Wang, X.; Liu, J. Effective PDT/PTT dual-modal phototherapeutic killing of pathogenic bacteria by using ruthenium nanoparticles. *J. Mater. Chem. B* **2016**, *4*, 6258–6270.
- (201) Jin, C.; Su, K.; Tan, L.; Liu, X.; Cui, Z.; Yang, X.; Li, Z.; Liang, Y.; Zhu, S.; Yeung, K. W. K.; Wu, S. Near-infrared light photocatalysis and photothermy of carbon quantum dots and au nanoparticles loaded titania nanotube array. *Mater. Des.* **2019**, *177*, 107845.
- (202) Li, L.; Liu, Y.; Hao, P.; Wang, Z.; Fu, L.; Ma, Z.; Zhou, J. PEDOT nanocomposites mediated dual-modal photodynamic and photothermal targeted sterilization in both NIR I and II window. *Biomaterials* **2015**, *41*, 132–40.
- (203) Lu, Y.; Li, L.; Lin, Z.; Wang, L.; Lin, L.; Li, M.; Zhang, Y.; Yin, Q.; Xia, H. A New Treatment Modality for Rheumatoid Arthritis: Combined Photothermal and Photodynamic Therapy Using Cu₇S₄ Nanoparticles. *Adv. Healthcare Mater.* **2018**, *7*, 1800013.
- (204) Sun, J.; Song, L.; Fan, Y.; Tian, L.; Luan, S.; Niu, S.; Ren, L.; Ming, W.; Zhao, J. Synergistic Photodynamic and Photothermal Antibacterial Nanocomposite Membrane Triggered by Single NIR Light Source. *ACS Appl. Mater. Interfaces* **2019**, *11*, 26581–26589.
- (205) Wang, W.-N.; Pei, P.; Chu, Z.-Y.; Chen, B.-J.; Qian, H.-S.; Zha, Z.-B.; Zhou, W.; Liu, T.; Shao, M.; Wang, H. Bi₂S₃ coated Au nanorods for enhanced photodynamic and photothermal antibacterial activities under NIR light. *Chem. Eng. J.* **2020**, *397*, 125488.
- (206) Wu, Q.; Wei, G.; Xu, Z.; Han, J.; Xi, J.; Fan, L.; Gao, L. Mechanistic Insight into the Light-Irradiated Carbon Capsules as an Antibacterial Agent. *ACS Appl. Mater. Interfaces* **2018**, *10*, 25026–25036.
- (207) Xu, X.; Liu, X.; Tan, L.; Cui, Z.; Yang, X.; Zhu, S.; Li, Z.; Yuan, X.; Zheng, Y.; Yeung, K. W. K.; Chu, P. K.; Wu, S. Controlled-temperature photothermal and oxidative bacteria killing and acceleration of wound healing by polydopamine-assisted Au-hydroxyapatite nanorods. *Acta Biomater.* **2018**, *77*, 352–364.
- (208) Zhang, X.; Liu, M.; Kang, Z.; Wang, B.; Wang, B.; Jiang, F.; Wang, X.; Yang, D.-P.; Luque, R. NIR-triggered photocatalytic/photothermal/photodynamic water remediation using eggshell-derived CaCO₃/CuS nanocomposites. *Chem. Eng. J.* **2020**, *388*, 124304.
- (209) Yu, Z. H.; Li, X.; Xu, F.; Hu, X. L.; Yan, J.; Kwon, N.; Chen, G. R.; Tang, T.; Dong, X.; Mai, Y.; Chen, D.; Yoon, J.; He, X. P.; Tian, H. A Supramolecular-Based Dual-Wavelength Phototherapeutic Agent with Broad-Spectrum Antimicrobial Activity Against Drug-Resistant Bacteria. *Angew. Chem., Int. Ed.* **2020**, *59*, 3658–3664.
- (210) Liang, Y.; Zhang, H.; Yuan, H.; Lu, W.; Li, Z.; Wang, L.; Gao, L.-H. Conjugated Polymer and Triphenylamine Derivative Codoped Nanoparticles for Photothermal and Photodynamic Antimicrobial Therapy. *ACS Appl. Bio Mater.* **2020**, *3*, 3494–3499.
- (211) Peng, R.; Luo, Y.; Cui, Q.; Wang, J.; Li, L. Near-Infrared Conjugated Oligomer for Effective Killing of Bacterial through Combination of Photodynamic and Photothermal Treatment. *ACS Appl. Bio Mater.* **2020**, *3*, 1305–1311.
- (212) Cui, Q.; Yuan, H.; Bao, X.; Ma, G.; Wu, M.; Xing, C. Synergistic Photodynamic and Photothermal Antibacterial Therapy Based on a Conjugated Polymer Nanoparticle-Doped Hydrogel. *ACS Appl. Bio Mater.* **2020**, *3*, 4436–4443.
- (213) Gao, D. Y.; Ji, X.; Wang, J. L.; Wang, Y. T.; Li, D. L.; Liu, Y. B.; Chang, K. W.; Qu, J. L.; Zheng, J.; Yuan, Z. Engineering a protein-based nanoplatfom as an antibacterial agent for light activated dual-modal photothermal and photodynamic therapy of infection in both the NIR I and II windows. *J. Mater. Chem. B* **2018**, *6*, 732–739.
- (214) Yin, M.; Li, Z.; Ju, E.; Wang, Z.; Dong, K.; Ren, J.; Qu, X. Multifunctional upconverting nanoparticles for near-infrared triggered and synergistic antibacterial resistance therapy. *Chem. Commun.* **2014**, *50*, 10488–90.
- (215) Zhou, K.; Qiu, X.; Xu, L.; Li, G.; Rao, B.; Guo, B.; Pei, D.; Li, A.; He, G. Poly(selenoviologen)-Assembled Upconversion Nanoparticles for Low-Power Single-NIR Light-Triggered Synergistic Photodynamic and Photothermal Antibacterial Therapy. *ACS Appl. Mater. Interfaces* **2020**, *12*, 26432–26443.
- (216) Yu, X.; He, D.; Zhang, X.; Zhang, H.; Song, J.; Shi, D.; Fan, Y.; Luo, G.; Deng, J. Surface-Adaptive and Initiator-Loaded Graphene as a Light-Induced Generator with Free Radicals for Drug-Resistant Bacteria Eradication. *ACS Appl. Mater. Interfaces* **2019**, *11*, 1766–1781.
- (217) Zhou, S.; Wang, Z.; Wang, Y.; Feng, L. Near-Infrared Light-Triggered Synergistic Phototherapy for Antimicrobial Therapy. *ACS Appl. Bio Mater.* **2020**, *3*, 1730–1737.
- (218) Hou, S.; Mahadevegowda, S. H.; Mai, V. C.; Chan-Park, M. B.; Duan, H. Glycosylated Copper Sulfide Nanocrystals for Targeted Photokilling of Bacteria in the Near-Infrared II Window. *Adv. Ther.* **2019**, *2*, 1900052.
- (219) Deng, T.; Zhao, H.; Shi, M.; Qiu, Y.; Jiang, S.; Yang, X.; Zhao, Y.; Zhang, Y. Photoactivated Trifunctional Platinum Nanobiotics for Precise Synergism of Multiple Antibacterial Modes. *Small* **2019**, *15*, 1902647.
- (220) Tong, C.; Zhong, X.; Yang, Y.; Liu, X.; Zhong, G.; Xiao, C.; Liu, B.; Wang, W.; Yang, X. PB@PDA@Ag nanosystem for synergistically eradicating MRSA and accelerating diabetic wound healing assisted with laser irradiation. *Biomaterials* **2020**, *243*, 119936.
- (221) Yin, Q.; Tan, L.; Lang, Q.; Ke, X.; Bai, L.; Guo, K.; Qiao, R.; Bai, S. Plasmonic molybdenum oxide nanosheets supported silver nanocubes for enhanced near-infrared antibacterial activity: Synergism of photothermal effect, silver release and photocatalytic reactions. *Appl. Catal., B* **2018**, *224*, 671–680.
- (222) Yuan, Z.; Lin, C.; He, Y.; Tao, B.; Chen, M.; Zhang, J.; Liu, P.; Cai, K. Near-Infrared Light-Triggered Nitric-Oxide-Enhanced Photodynamic Therapy and Low-Temperature Photothermal Therapy for Biofilm Elimination. *ACS Nano* **2020**, *14*, 3546–3562.
- (223) Li, Y.; Liu, X.; Tan, L.; Cui, Z.; Yang, X.; Zheng, Y.; Yeung, K. W. K.; Chu, P. K.; Wu, S. Rapid Sterilization and Accelerated Wound Healing Using Zn²⁺ and Graphene Oxide Modified g-C₃N₄ under Dual Light Irradiation. *Adv. Funct. Mater.* **2018**, *28*, 1800299.
- (224) Li, Y.; Liu, X.; Tan, L.; Cui, Z.; Jing, D.; Yang, X.; Liang, Y.; Li, Z.; Zhu, S.; Zheng, Y.; Yeung, K. W. K.; Zheng, D.; Wang, X.; Wu, S. Eradicating Multidrug-Resistant Bacteria Rapidly Using a Multi Functional g-C₃N₄@Bi₂S₃ Nanorod Heterojunction with or without Antibiotics. *Adv. Funct. Mater.* **2019**, *29*, 1900946.
- (225) Hu, X. L.; Chu, L.; Dong, X.; Chen, G. R.; Tang, T.; Chen, D.; He, X. P.; Tian, H. Multivalent Glycosheets for Double Light-Driven

Therapy of Multidrug-Resistant Bacteria on Wounds. *Adv. Funct. Mater.* **2019**, *29*, 1806986.

(226) Nguyen, T. T. T.; Ghosh, C.; Hwang, S.-G.; Tran, L. D.; Park, J. S. Characteristics of curcumin-loaded poly (lactic acid) nanofibers for wound healing. *J. Mater. Sci.* **2013**, *48*, 7125–7133.

(227) Azadmanjiri, J.; Wang, J.; Berndt, C. C.; Yu, A. 2D layered organic–inorganic heterostructures for clean energy applications. *J. Mater. Chem. A* **2018**, *6*, 3824–3849.

(228) Zhang, Q.; Liu, X.; Tan, L.; Cui, Z.; Li, Z.; Liang, Y.; Zhu, S.; Yeung, K. W. K.; Zheng, Y.; Wu, S. An UV to NIR-driven platform based on red phosphorus/graphene oxide film for rapid microbial inactivation. *Chem. Eng. J.* **2020**, *383*, 123088.

(229) Ray, J. R.; Tadepalli, S.; Nergiz, S. Z.; Liu, K. K.; You, L.; Tang, Y.; Singamaneni, S.; Jun, Y. S. Hydrophilic, bactericidal nanoheater-enabled reverse osmosis membranes to improve fouling resistance. *ACS Appl. Mater. Interfaces* **2015**, *7*, 11117–26.

(230) Luo, J.; Deng, W.; Yang, F.; Wu, Z.; Huang, M.; Gu, M. Gold nanoparticles decorated graphene oxide/nanocellulose paper for NIR laser-induced photothermal ablation of pathogenic bacteria. *Carbohydr. Polym.* **2018**, *198*, 206–214.

(231) Li, Y.; Li, N.; Ge, J.; Xue, Y.; Niu, W.; Chen, M.; Du, Y.; Ma, P. X.; Lei, B. Biodegradable thermal imaging-tracked ultralong nanowire-reinforced conductive nanocomposites elastomers with intrinsic efficient antibacterial and anticancer activity for enhanced biomedical application potential. *Biomaterials* **2019**, *201*, 68–76.

(232) Lei, W.; Ren, K.; Chen, T.; Chen, X.; Li, B.; Chang, H.; Ji, J. Polydopamine Nanocoating for Effective Photothermal Killing of Bacteria and Fungus upon Near-Infrared Irradiation. *Adv. Mater. Interfaces* **2016**, *3*, 1600767.

(233) Kim, S. H.; Kang, E. B.; Jeong, C. J.; Sharker, S. M.; In, I.; Park, S. Y. Light controllable surface coating for effective photothermal killing of bacteria. *ACS Appl. Mater. Interfaces* **2015**, *7*, 15600–6.

(234) Khantamat, O.; Li, C. H.; Yu, F.; Jamison, A. C.; Shih, W. C.; Cai, C.; Lee, T. R. Gold nanoshell-decorated silicone surfaces for the near-infrared (NIR) photothermal destruction of the pathogenic bacterium *E. faecalis*. *ACS Appl. Mater. Interfaces* **2015**, *7*, 3981–93.

(235) Hui, L.; Auletta, J. T.; Huang, Z.; Chen, X.; Xia, F.; Yang, S.; Liu, H.; Yang, L. Surface Disinfection Enabled by a Layer-by-Layer Thin Film of Polyelectrolyte-Stabilized Reduced Graphene Oxide upon Solar Near-Infrared Irradiation. *ACS Appl. Mater. Interfaces* **2015**, *7*, 10511–7.

(236) Qiao, B.; Pang, Q.; Yuan, P.; Luo, Y.; Ma, L. Smart wound dressing for infection monitoring and NIR-triggered antibacterial treatment. *Biomater. Sci.* **2020**, *8*, 1649–1657.

(237) Xi, Y.; Ge, J.; Wang, M.; Chen, M.; Niu, W.; Cheng, W.; Xue, Y.; Lin, C.; Lei, B. Bioactive Anti-inflammatory, Antibacterial, Antioxidative Silicon-Based Nanofibrous Dressing Enables Cutaneous Tumor Photothermo-Chemo Therapy and Infection-Induced Wound Healing. *ACS Nano* **2020**, *14*, 2904–2916.

(238) Zhao, Y. Q.; Sun, Y.; Zhang, Y.; Ding, X.; Zhao, N.; Yu, B.; Zhao, H.; Duan, S.; Xu, F. J. Well-Defined Gold Nanorod/Polymer Hybrid Coating with Inherent Antifouling and Photothermal Bactericidal Properties for Treating an Infected Hernia. *ACS Nano* **2020**, *14*, 2265–2275.

(239) Budimir, M.; Jijie, R.; Ye, R.; Barras, A.; Melinte, S.; Silhanek, A.; Markovic, Z.; Szunerits, S.; Boukherroub, R. Efficient capture and photothermal ablation of planktonic bacteria and biofilms using reduced graphene oxide-polyethyleneimine flexible nanoheaters. *J. Mater. Chem. B* **2019**, *7*, 2771–2781.

(240) Kim, Y. K.; Kang, E. B.; Kim, S. M.; Park, C. P.; In, I.; Park, S. Y. Performance of NIR-Mediated Antibacterial Continuous Flow Microreactors Prepared by Mussel-Inspired Immobilization of Cs_{0.33}WO₃ Photothermal Agents. *ACS Appl. Mater. Interfaces* **2017**, *9*, 3192–3200.

(241) Qu, Y.; Wei, T.; Zhao, J.; Jiang, S.; Yang, P.; Yu, Q.; Chen, H. Regenerable smart antibacterial surfaces: full removal of killed bacteria via a sequential degradable layer. *J. Mater. Chem. B* **2018**, *6*, 3946–3955.

(242) Wang, Y.; Wei, T.; Qu, Y.; Zhou, Y.; Zheng, Y.; Huang, C.; Zhang, Y.; Yu, Q.; Chen, H. Smart, Photothermally Activated,

Antibacterial Surfaces with Thermally Triggered Bacteria-Releasing Properties. *ACS Appl. Mater. Interfaces* **2020**, *12*, 21283–21291.

(243) Ferguson, R. J.; Palmer, A. J. R.; Taylor, A.; Porter, M. L.; Malchau, H.; Glyn-Jones, S. Hip replacement. *Lancet* **2018**, *392*, 1662–1671.

(244) Nagpal, A.; Baddour, L. M.; Sohail, M. R. Microbiology and Pathogenesis of Cardiovascular Implantable Electronic Device Infections. *Circ.: Arrhythmia Electrophysiol.* **2012**, *5*, 433–441.

(245) Cheng, K. H.; Leung, S. L.; Hoekman, H. W.; Beekhuis, W. H.; Mulder, P. G. H.; Geerards, A. J. M.; Kijlstra, A. Incidence of contact-lens-associated microbial keratitis and its related morbidity. *Lancet* **1999**, *354*, 181–185.

(246) Puhto, A.-P.; Puhto, T. M.; Niinimäki, T. T.; Leppilähti, J. I.; Syrjälä, H. P. T. Two-Stage Revision for Prosthetic Joint Infection: Outcome and Role of Reimplantation Microbiology in 107 Cases. *J. Arthroplasty* **2014**, *29*, 1101–1104.

(247) Lichter, J. A.; Van Vliet, K. J.; Rubner, M. F. Design of Antibacterial Surfaces and Interfaces: Polyelectrolyte Multilayers as a Multifunctional Platform. *Macromolecules* **2009**, *42*, 8573–8586.

(248) Wang, W.; Cheng, X.; Liao, J.; Lin, Z.; Chen, L.; Liu, D.; Zhang, T.; Li, L.; Lu, Y.; Xia, H. Synergistic Photothermal and Photodynamic Therapy for Effective Implant-Related Bacterial Infection Elimination and Biofilm Disruption Using Cu₉S₈ Nanoparticles. *ACS Biomater. Sci. Eng.* **2019**, *5*, 6243–6253.

(249) Song, J.; Liu, H.; Lei, M.; Tan, H.; Chen, Z.; Antoshin, A.; Payne, G. F.; Qu, X.; Liu, C. Redox-Channelling Polydopamine-Ferrocene (PDA-Fc) Coating To Confer Context-Dependent and Photothermal Antimicrobial Activities. *ACS Appl. Mater. Interfaces* **2020**, *12*, 8915–8928.

(250) Li, M.; Li, L.; Su, K.; Liu, X.; Zhang, T.; Liang, Y.; Jing, D.; Yang, X.; Zheng, D.; Cui, Z.; Li, Z.; Zhu, S.; Yeung, K. W. K.; Zheng, Y.; Wang, X.; Wu, S. Highly Effective and Noninvasive Near-Infrared Eradication of a *Staphylococcus aureus* Biofilm on Implants by a Photoresponsive Coating within 20 min. *Adv. Sci.* **2019**, *6*, 1900599.

(251) Wang, X.; Tan, L.; Liu, X.; Cui, Z.; Yang, X.; Yeung, K. W. K.; Chu, P. K.; Wu, S. Construction of perfluorohexane/IR780@liposome coating on Ti for rapid bacteria killing under permeable near infrared light. *Biomater. Sci.* **2018**, *6*, 2460–2471.

(252) Zhang, W.; Yang, C.; Lei, Z.; Guan, G.; He, S. A.; Zhang, Z.; Zou, R.; Shen, H.; Hu, J. New Strategy for Specific Eradication of Implant-Related Infections Based on Special and Selective Degradability of Rhenium Trioxide Nanocubes. *ACS Appl. Mater. Interfaces* **2019**, *11*, 25691–25701.

(253) Zhao, S.; Xu, Y.; Xu, W.; Weng, Z.; Cao, F.; Wan, X.; Cui, T.; Yu, Y.; Liao, L.; Wang, X. Tremella-Like ZnO@Col-I-Decorated Titanium Surfaces with Dual-Light-Defined Broad-Spectrum Antibacterial and Triple Osteogenic Properties. *ACS Appl. Mater. Interfaces* **2020**, *12*, 30044–30051.

(254) Deng, Y.; Gao, X.; Shi, X.-L.; Lu, S.; Yang, W.; Duan, C.; Chen, Z.-G. Graphene Oxide and Adiponectin-Functionalized Sulfonated Poly(etheretherketone) with Effective Osteogenicity and Remotely Repeatable Photodisinfection. *Chem. Mater.* **2020**, *32*, 2180–2193.

(255) Wang, X.; Su, K.; Tan, L.; Liu, X.; Cui, Z.; Jing, D.; Yang, X.; Liang, Y.; Li, Z.; Zhu, S.; Yeung, K. W. K.; Zheng, D.; Wu, S. Rapid and Highly Effective Noninvasive Disinfection by Hybrid Ag/CS@MnO₂ Nanosheets Using Near-Infrared Light. *ACS Appl. Mater. Interfaces* **2019**, *11*, 15014–15027.

(256) Li, Y.; Liu, X.; Li, B.; Zheng, Y.; Han, Y.; Chen, D. F.; Yeung, K. W. K.; Cui, Z.; Liang, Y.; Li, Z.; Zhu, S.; Wang, X.; Wu, S. Near-Infrared Light Triggered Phototherapy and Immunotherapy for Elimination of Methicillin-Resistant *Staphylococcus aureus* Biofilm Infection on Bone Implant. *ACS Nano* **2020**, *14*, 8157–8170.

(257) Feng, Z.; Liu, X.; Tan, L.; Cui, Z.; Yang, X.; Li, Z.; Zheng, Y.; Yeung, K. W. K.; Wu, S. Electrophoretic Deposited Stable Chitosan@MoS₂ Coating with Rapid In Situ Bacteria-Killing Ability under Dual-Light Irradiation. *Small* **2018**, *14*, 1704347.

(258) Tan, L.; Li, J.; Liu, X.; Cui, Z.; Yang, X.; Zhu, S.; Li, Z.; Yuan, X.; Zheng, Y.; Yeung, K. W. K.; Pan, H.; Wang, X.; Wu, S. Rapid Biofilm

Eradication on Bone Implants Using Red Phosphorus and Near-Infrared Light. *Adv. Mater.* **2018**, *30*, 1801808.

(259) Hong, L.; Liu, X.; Tan, L.; Cui, Z.; Yang, X.; Liang, Y.; Li, Z.; Zhu, S.; Zheng, Y.; Yeung, K. W. K.; Jing, D.; Zheng, D.; Wang, X.; Wu, S. Rapid Biofilm Elimination on Bone Implants Using Near-Infrared-Activated Inorganic Semiconductor Heterostructures. *Adv. Healthcare Mater.* **2019**, *8*, 1900835.

(260) Yuan, Z.; Tao, B.; He, Y.; Mu, C.; Liu, G.; Zhang, J.; Liao, Q.; Liu, P.; Cai, K. Remote eradication of biofilm on titanium implant via near-infrared light triggered photothermal/photodynamic therapy strategy. *Biomaterials* **2019**, *223*, 119479.

(261) Yuan, H.; Zhan, Y.; Rowan, A. E.; Xing, C.; Kouwer, P. H. J. Biomimetic Networks with Enhanced Photodynamic Antimicrobial Activity from Conjugated Polythiophene/Polysocyanide Hybrid Hydrogels. *Angew. Chem., Int. Ed.* **2020**, *59*, 2720–2724.

(262) Guo, J.; Xing, C.; Yuan, H.; Chai, R.; Zhan, Y. Oligo (p-Phenylene Vinylene)/Polysocyanopeptide Biomimetic Composite Hydrogel-Based Three-Dimensional Cell Culture System for Anti-cancer and Antibacterial Therapeutics. *ACS Appl. Bio Mater.* **2019**, *2*, 2520–2527.

(263) Döring, A.; Birnbaum, W.; Kuckling, D. Responsive hydrogels – structurally and dimensionally optimized smart frameworks for applications in catalysis, micro-system technology and material science. *Chem. Soc. Rev.* **2013**, *42*, 7391–7420.

(264) Xu, M. L.; Guan, L. Y.; Li, S. K.; Chen, L.; Chen, Z. Stable gold graphitic nanocapsule doped hydrogels for efficient photothermal antibacterial applications. *Chem. Commun.* **2019**, *55*, 5359–5362.

(265) Mai, B.; Jia, M.; Liu, S.; Sheng, Z.; Li, M.; Gao, Y.; Wang, X.; Liu, Q.; Wang, P. Smart Hydrogel-Based DVDMS/bFGF Nanohybrids for Antibacterial Phototherapy with Multiple Damaging Sites and Accelerated Wound Healing. *ACS Appl. Mater. Interfaces* **2020**, *12*, 10156–10169.

(266) Liu, Y.; Xiao, Y.; Cao, Y.; Guo, Z.; Li, F.; Wang, L. Construction of Chitosan-Based Hydrogel Incorporated with Antimonene Nano-sheets for Rapid Capture and Elimination of Bacteria. *Adv. Funct. Mater.* **2020**, *30*, 2003196.

(267) Liu, Y.; Li, F.; Guo, Z.; Xiao, Y.; Zhang, Y.; Sun, X.; Zhe, T.; Cao, Y.; Wang, L.; Lu, Q.; Wang, J. Silver nanoparticle-embedded hydrogel as a photothermal platform for combating bacterial infections. *Chem. Eng. J.* **2020**, *382*, 122990.

(268) Li, M.; Liu, X.; Tan, L.; Cui, Z.; Yang, X.; Li, Z.; Zheng, Y.; Yeung, K. W. K.; Chu, P. K.; Wu, S. Noninvasive rapid bacteria-killing and acceleration of wound healing through photothermal/photodynamic/copper ion synergistic action of a hybrid hydrogel. *Biomater. Sci.* **2018**, *6*, 2110–2121.

(269) Chen, S.; Tang, F.; Tang, L.; Li, L. Synthesis of Cu-Nanoparticle Hydrogel with Self-Healing and Photothermal Properties. *ACS Appl. Mater. Interfaces* **2017**, *9*, 20895–20903.

(270) Zhang, C.; Wu, B.; Zhou, Y.; Zhou, F.; Liu, W.; Wang, Z. Mussel-inspired hydrogels: from design principles to promising applications. *Chem. Soc. Rev.* **2020**, *49*, 3605–3637.

(271) Hsiao, C.-W.; Chen, H.-L.; Liao, Z.-X.; Sureshbabu, R.; Hsiao, H.-C.; Lin, S.-J.; Chang, Y.; Sung, H.-W. Effective Photothermal Killing of Pathogenic Bacteria by Using Spatially Tunable Colloidal Gels with Nano-Localized Heating Sources. *Adv. Funct. Mater.* **2015**, *25*, 721–728.

(272) Abdou Mohamed, M. A.; Raeesi, V.; Turner, P. V.; Rebbapragada, A.; Banks, K.; Chan, W. C. A versatile plasmonic thermogel for disinfection of antimicrobial resistant bacteria. *Biomaterials* **2016**, *97*, 154–63.

(273) Ko, Y.; Kim, J.; Jeong, H. Y.; Kwon, G.; Kim, D.; Ku, M.; Yang, J.; Yamauchi, Y.; Kim, H. Y.; Lee, C.; You, J. Antibacterial poly (3,4-ethylenedioxythiophene):poly(styrene-sulfonate)/agarose nanocomposite hydrogels with thermo-processability and self-healing. *Carbohydr. Polym.* **2019**, *203*, 26–34.

(274) Wang, J.; Chen, X. Y.; Zhao, Y.; Yang, Y.; Wang, W.; Wu, C.; Yang, B.; Zhang, Z.; Zhang, L.; Liu, Y.; Du, X.; Li, W.; Qiu, L.; Jiang, P.; Mou, X. Z.; Li, Y. Q. pH-Switchable Antimicrobial Nanofiber Networks

of Hydrogel Eradicate Biofilm and Rescue Stalled Healing in Chronic Wounds. *ACS Nano* **2019**, *13*, 11686–11697.

(275) Yu, Y.; Li, P.; Zhu, C.; Ning, N.; Zhang, S.; Vancso, G. J. Multifunctional and Recyclable Photothermally Responsive Cryogels as Efficient Platforms for Wound Healing. *Adv. Funct. Mater.* **2019**, *29*, 1904402.

(276) Deng, H.; Yu, Z.; Chen, S.; Fei, L.; Sha, Q.; Zhou, N.; Chen, Z.; Xu, C. Facile and eco-friendly fabrication of polysaccharides-based nanocomposite hydrogel for photothermal treatment of wound infection. *Carbohydr. Polym.* **2020**, *230*, 115565.

(277) Zhou, L.; Xi, Y.; Xue, Y.; Wang, M.; Liu, Y.; Guo, Y.; Lei, B. Injectable Self-Healing Antibacterial Bioactive Polypeptide-Based Hybrid Nanosystems for Efficiently Treating Multidrug Resistant Infection, Skin-Tumor Therapy, and Enhancing Wound Healing. *Adv. Funct. Mater.* **2019**, *29*, 1806883.

(278) Zhao, X.; Liang, Y.; Huang, Y.; He, J.; Han, Y.; Guo, B. Physical Double-Network Hydrogel Adhesives with Rapid Shape Adaptability, Fast Self-Healing, Antioxidant and NIR/pH Stimulus-Responsiveness for Multidrug-Resistant Bacterial Infection and Removable Wound Dressing. *Adv. Funct. Mater.* **2020**, *30*, 1910748.

(279) Han, D.; Li, Y.; Liu, X.; Li, B.; Han, Y.; Zheng, Y.; Yeung, K. W. K.; Li, C.; Cui, Z.; Liang, Y.; Li, Z.; Zhu, S.; Wang, X.; Wu, S. Rapid bacteria trapping and killing of metal-organic frameworks strengthened photo-responsive hydrogel for rapid tissue repair of bacterial infected wounds. *Chem. Eng. J.* **2020**, *396*, 125194.

(280) Zhao, X.; Guo, B.; Wu, H.; Liang, Y.; Ma, P. X. Injectable antibacterial conductive nanocomposite cryogels with rapid shape recovery for noncompressible hemorrhage and wound healing. *Nat. Commun.* **2018**, *9*, 2784.

(281) Hu, B.; Berkey, C.; Feliciano, T.; Chen, X.; Li, Z.; Chen, C.; Amini, S.; Nai, M. H.; Lei, Q. L.; Ni, R.; Wang, J.; Leow, W. R.; Pan, S.; Li, Y. Q.; Cai, P.; Miserez, A.; Li, S.; Lim, C. T.; Wu, Y. L.; Odom, T. W.; Dauskardt, R. H.; Chen, X. Thermal-Disrupting Interface Mitigates Intercellular Cohesion Loss for Accurate Topical Antibacterial Therapy. *Adv. Mater.* **2020**, *32*, 1907030.